CHEMISTRY
A EUROPEAN JOURNAL

FULL PAPER

DOI: 10.1002/chem.201203983

Interlocked Porphyrin Switches

Ruud G. E. Coumans, Johannes A. A. W. Elemans,* Alan E. Rowan,* and Roeland J. M. Nolte*[a]

Abstract: We describe the synthesis of a series of interlocked structures from porphyrin–glycoluril cage compounds and bis(olefin)-terminated viologens by an olefin-metathesis protocol. The length of the chain connecting the olefin substituents with the viologen has a marked effect on the products of the ring-closure reaction. Long chains give [2]- and [3]catenane structures, whereas short chains give a mixture of [3]-, [4]-, and [5]catenanes. For comparison several [2]rotaxane compounds were prepared. The interlocked catenane and rotaxane structures display switching behavior, which can be controlled by the addition of acid and base. The kinetic and thermodynamic parameters of the switching processes have been determined by NMR spectroscopy.

Keywords: catenanes · interlocked structures · olefin metathesis · porphyrins · rotaxanes · switches

Introduction

The development and study of mechanically interlocked compounds such as rotaxanes, catenanes, molecular necklaces, and Borromean rings remains a fascinating area of supramolecular chemistry.[1] These interlocked architectures have shown to be potential candidates for incorporation into molecular memory devices owing to their tunable switching (on/off) behavior. The research group of Stoddart has demonstrated that it is possible to immobilize switchable [2]catenanes onto a surface, while retaining their switching behavior, resulting in prototypical molecular memories.[2] The same group has more recently shown that certain [3]rotaxanes, when grafted onto a thin metal surface, are capable of bending the surface as a result of electrochemically induced mechanical contraction of the rotaxanes.[3] These examples clearly demonstrate that interlocked molecules are promising building blocks and have the potential to be applied as functional elements in nanotechnology.[4] These studies stimulated us to investigate interlocked structures that contain one or more functional components, namely, porphyrins, as part of a project aimed at developing a molecular device that can perform actions on a polymer tape according to instructions from a tape head.[5] The blueprint is shown in Figure 1. As a tape, polymers will be used containing sites that can be chemically transformed, for example, alkene double bonds in polybutadiene that can be converted into epoxide functions.[6] The tape head will be a glycoluril double cage compound containing two metal porphyrin cages that are held together by a ligand bond (1,4-diazabicyclo[2.2.2]octane) and by hydrogen-bonding interactions. In a previous paper, we have shown that, in this compound, information can be transferred from one porphyrin cage to the other by four positive allosteric interactions.[7] For this concept to be realised, one of the cages will contain a ring compound, that is, a catenane, that can rotate and provide the instructions. The other cage will be threaded onto a polymer chain (see Figure 1).[8] As a first step in the construction of such a molecular device, we decided to study the synthesis of a porphyrin–glycoluril rotaxane using olefin metathesis. We have already demonstrated that olefin metathesis in combination with the selective recognition of viologens by porphyrin–glycoluril host **1** (Scheme 1) is an excellent way to synthesize rotaxanes.[9] This stimulated us to further explore this approach and use it for the synthesis of porphyrin-based catenanes that might function as simple molecular switches. Here, the synthesis and (photo)physical

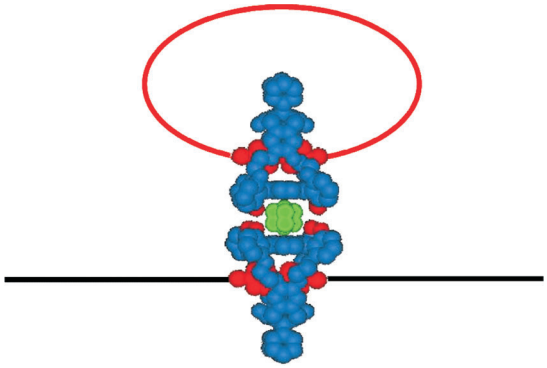

Figure 1. A molecular device in which information is transferred from a catenane ring (red oval) to a polymer chain (black line).

[a] Dr. R. G. E. Coumans, Dr. J. A. A. W. Elemans, Prof. A. E. Rowan, Prof. R. J. M. Nolte
Radboud University Nijmegen
Institute for Molecules and Materials
Heyendaalseweg 135, 6525 AJ Nijmegen (The Netherlands)
Fax: (+31) 24-3652929
E-mail: J.Elemans@science.ru.nl
A.Rowan@science.ru.nl
R.Nolte@science.ru.nl

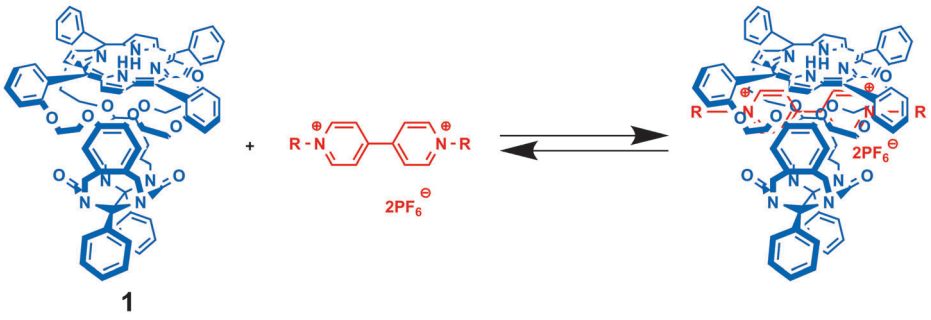

Scheme 1. Formation of a host–guest complex between the cavity-containing porphyrin **1** and a viologen guest.

properties of a variety of interlocked structures based on porphyrin host **1** are described.

Results and Discussion

Design: Our strategy to construct porphyrin-containing catenanes is based on an olefin-metathesis protocol, which was published previously by our research group.[9] In organic solvents, porphyrin host **1** forms very stable complexes with viologen (*N*,*N*′-dialkyl-4,4′-bipyridinium) derivatives (Scheme 1).[10] The strong binding of these guests relies on a combination of factors, namely, π–π stacking interactions between the aromatic surfaces of the viologen and **1**, electrostatic interactions between the positive charges on the guest and the crown ether moieties of **1**, and C–H···O hydrogen bonding between the α-bipyridinium protons and the crown ether and carbonyl oxygen atoms of **1**. When viologens that contain terminal olefins as N substituents are complexed in the cavity of **1**, the resulting host–guest complexes can in principle be subjected to olefin-metathesis reactions, so that interlocked porphyrin-containing species are generated. Similar olefin ring-closing and cross metathesis protocols have proven to be very effective for the high-yield synthesis of a variety of interlocked molecules.[11] Herein, we will make use of two olefin-containing viologens, **3** and **4** (see Scheme 2), which differ in the length of the bipyridine N substituents.

Synthesis of olefin-containing viologens: The synthesis of viologen **3** started with the etherification of 1,10-dibromodecane with 9-decenol using NaH as a base in THF, affording bromide derivative **2** in 44% yield after purification by column chromatography (Scheme 2). This compound was subsequently coupled to 4,4′-bipyridine in hot *N*,*N*-dimethylformamide (DMF), after which ion exchange with NH_4PF_6 in water gave **3** in 23% yield, after recrystallization from methanol. To obtain a viologen with a shorter substituent, 4,4′-bipyridine was reacted with an excess of 8-bromooctene in hot DMF, followed by ion-exchange with NH_4PF_6, to give viologen **4** in 61% yield.

Synthesis of catenanes: The mixing of porphyrin clip **1** with viologen **3** in $CHCl_3$/acetone (1:1, *v*/*v*), followed by precipitation of the product in *n*-hexane, quantitatively furnished [2]pseudorotaxane **5** (Scheme 3). Indicative for [2]pseudorotaxane formation are the large complexation-induced shifts observed in the ^{1}H NMR spectrum ($CDCl_3$) for the signals of the aromatic viologen protons, H_a ($\Delta\delta = -2.65$ ppm) and H_b ($\Delta\delta = -4.07$ ppm), shifts that are the result of shielding by the porphyrin macrocycle and the aromatic side walls of **1**. The complex was readily soluble in CH_2Cl_2, thus setting the stage for a ring-closing metathesis reaction (RCM) of the terminal alkene groups of the viologen by using the first generation Grubbs' catalyst, $[RuCHPh(Cl)_2(PCy_3)_2]$ (Scheme 3). To minimize intermolecular crosslinking, the reaction was performed under high-dilution conditions ([**5**] ≈0.0005 M). At these concentrations, more than 99% of **1** is

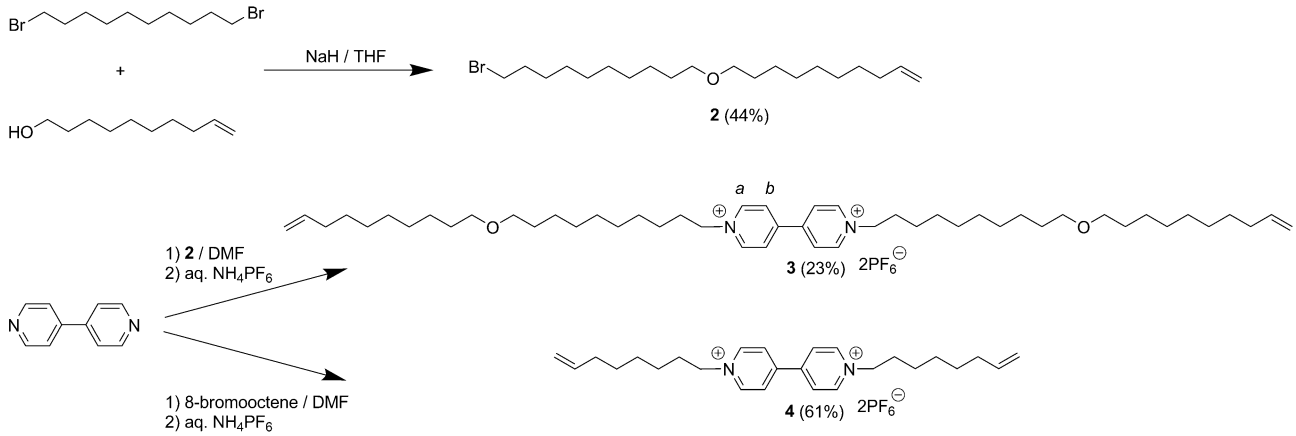

Scheme 2. Synthesis of olefin-terminated viologens.

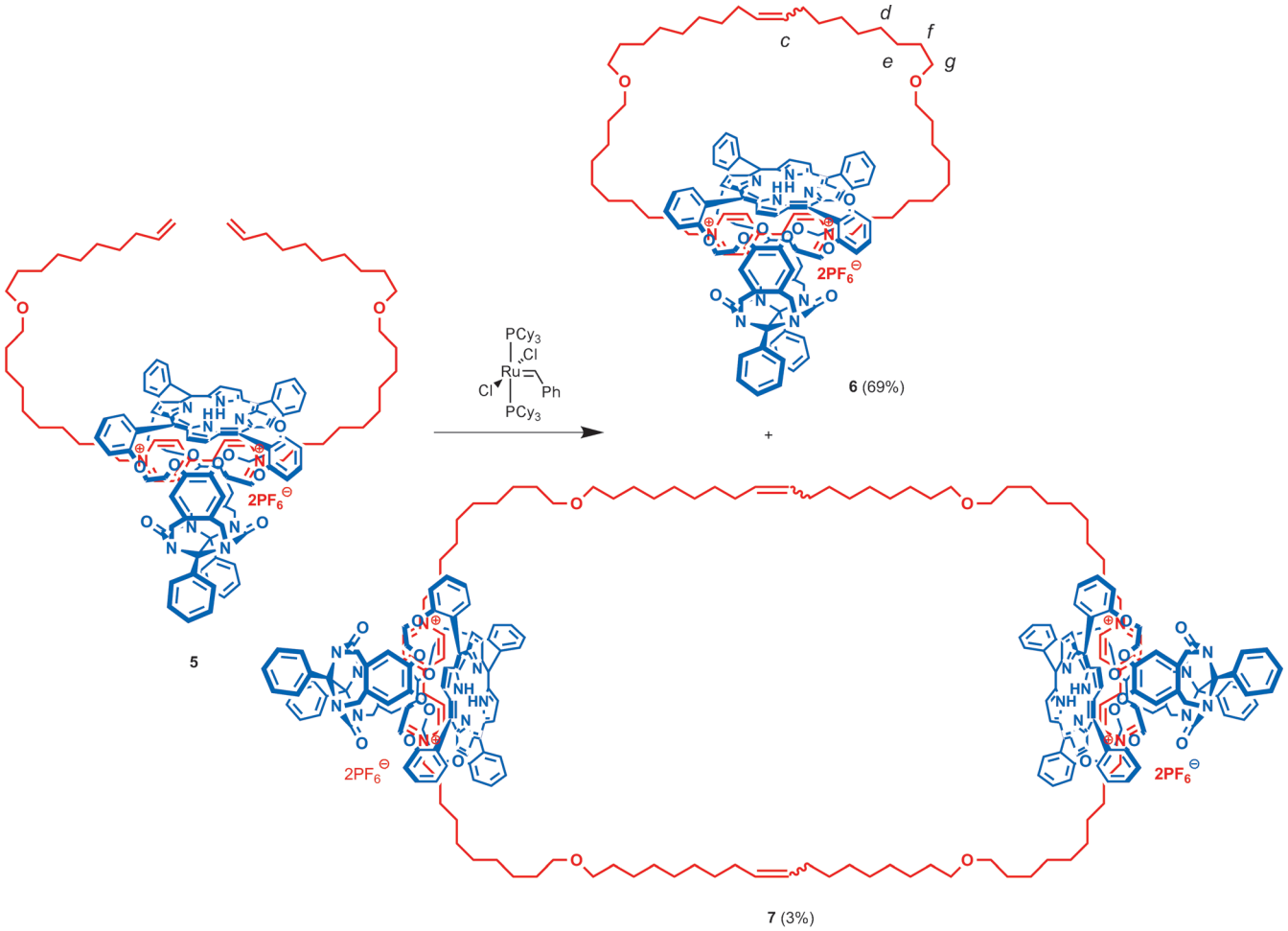

Scheme 3. Synthesis of [2]pseudorotaxane **5**, [2]catenane **6**, and [3]catenane **7**. Cy = cyclohexyl.

complexed by **3** because of the high association constant ($K_a \approx 10^7\,M^{-1}$). Subjecting a solution of **5** in CH_2Cl_2 to 20 mol% of Grubbs' catalyst for 24 hours at room temperature resulted in a mixture of products, of which [2]catenane **6** could be isolated in 69% yield after column chromatography, as a mixture of *E*/*Z* isomers in a 4:1 ratio. [3]Catenane **7** was also isolated in 3% yield, as a mixture of *E*/*E*, *E*/*Z* and *Z*/*Z* isomers (total *E*/*Z* ratio = 4:1). Both catenanes contain a very large macrocycle: a 48-membered ring in the case of **6** and a 96-membered one in the case of **7**.[12] The MALDI-TOF spectra of the [2]catenanes (Figure 2) showed peaks for **6** at *m*/*z* 2063.1 and 2208.1, corresponding to $[M-2PF_6]^+$ and $[M-PF_6]^+$, respectively, and four peaks for **7** at *m*/*z* 4125.6, 4271.6, 4416.4, and 4560.7, corresponding to $[M-nPF_6]^+$ ($n = 1$–4), respectively.

The 2D-NOESY spectrum of **6** revealed nOe contacts between the pyrrole NH protons of the porphyrin and the aromatic protons H_a and H_b (see Scheme 2) of the viologen, thus indicating that the latter moiety is situated inside the cavity of **1**. The resonances of the *trans*-alkene protons (H_c, Scheme 3) are shifted upfield to $\delta = 4.87$ ppm, ($\Delta\delta \approx -0.5$ ppm) compared to other internal alkenes, a characteristic that is attributed to shielding effects by either the por-

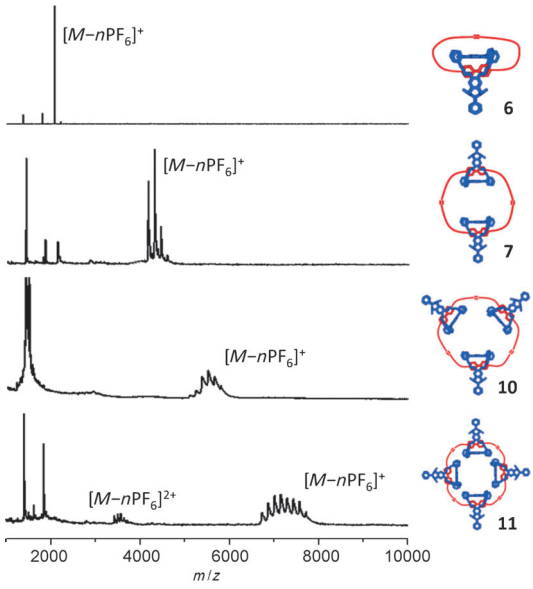

Figure 2. MALDI-TOF spectra of [2]catenane **6**, [3]catenane **7**, [4]catenane **10** and [5]catenane **11**.

phyrin macrocycle of **1**, the aromatic side walls of **1**, or both. In the ^{1}H NMR spectrum of [3]catenane **7**, the *trans*-alkene protons resonate at $\delta = 5.39$ ppm, thus indicating that the alkene parts of the thread are, in this case, situated further away from the aromatic surfaces of the host. To investigate the effect of spacer length on the outcome of the metathesis reaction, the same RCM reaction was repeated using viologen **4**, which has shorter N substituents. The desired [2]pseudorotaxane **8** was readily assembled according to the aforementioned procedure. Exposing a 0.001 M solution of **8** in CH_2Cl_2 to 20 mol% of Grubbs' catalyst in refluxing CH_2Cl_2 for 24 hours gave a mixture of products, containing [3]catenane **9**, [4]catenane **10**, [5]catenane **11**, and some higher cyclic oligomers (Scheme 4).[13] It appeared that refluxing the solution resulted in a much better conversion than performing the reaction at room temperature. The catenanes **10** and **11** could be isolated from the product mixture in 18% and 11% yield, respectively (~95% pure), using a combination of silica and size-exclusion chromatography. Catenane **9**, which was only formed in very low yield, could not be obtained pure. To the best of our knowledge, these are the first examples of porphyrin-containing [4]- and [5]catenanes.[14] MALDI-TOF spectra showed six peaks for catenane **10** at *m*/*z* 5088, 5225, 5370, 5516, 5661, and 5805, corresponding to $[M-n\mathrm{PF_6}]^+$ ($n = 1$–6) (Figure 2). For catenane **11**, MALDI-TOF spectra showed eight peaks at *m*/*z* 6778, 6923, 7068, 7213, 7358, 7503, 7648, 7793, corresponding to $[M-n\mathrm{PF_6}]^+$ ($n = 1$–8) (Figure 2). No formation of a [2]catenane was observed, even when the reaction was performed at higher dilution (0.0005 M), thus indicating that the N sub-

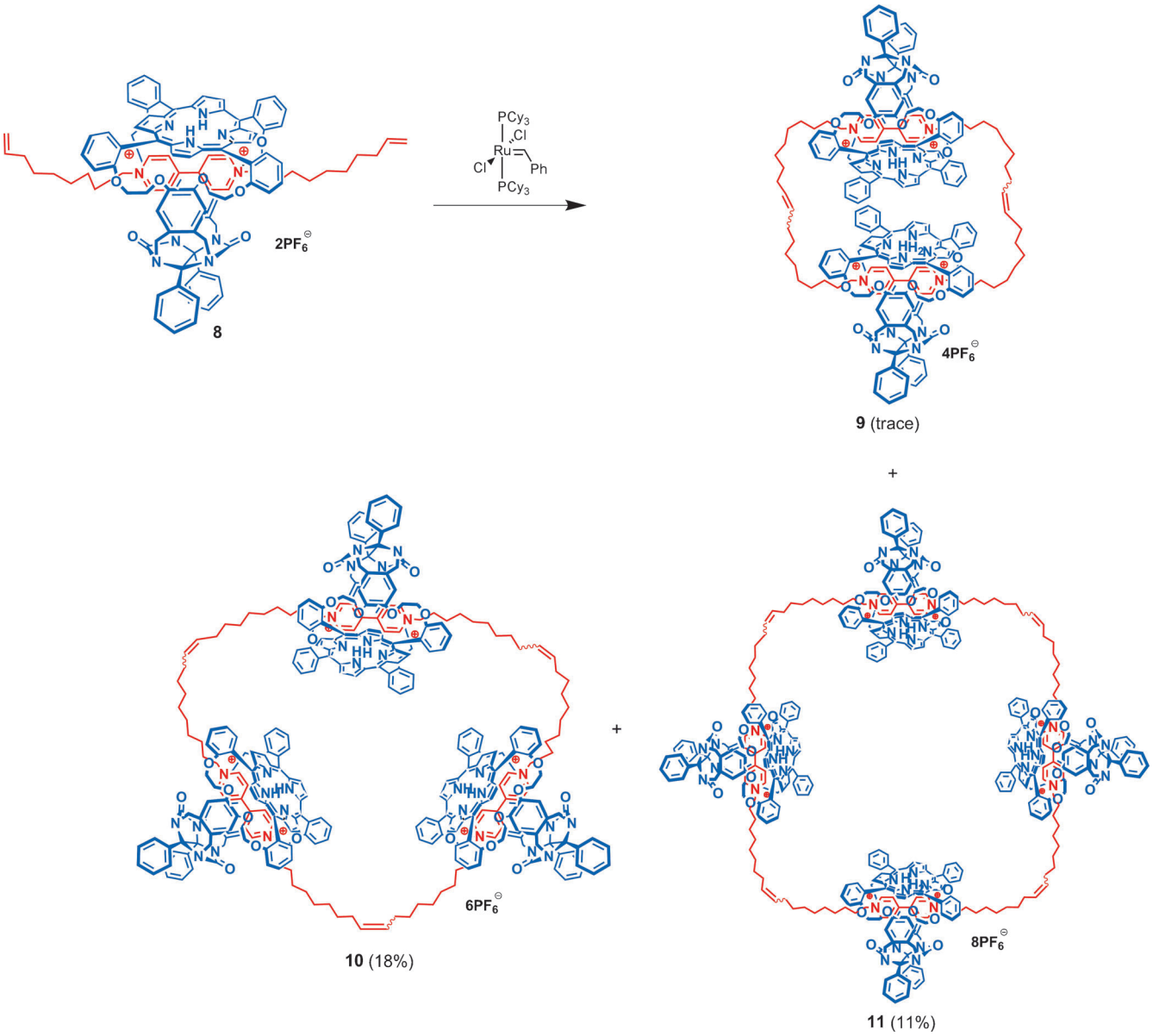

Scheme 4. Synthesis of [3]catenane **9**, [4]catenane **10**, and [5]catenane **11**.

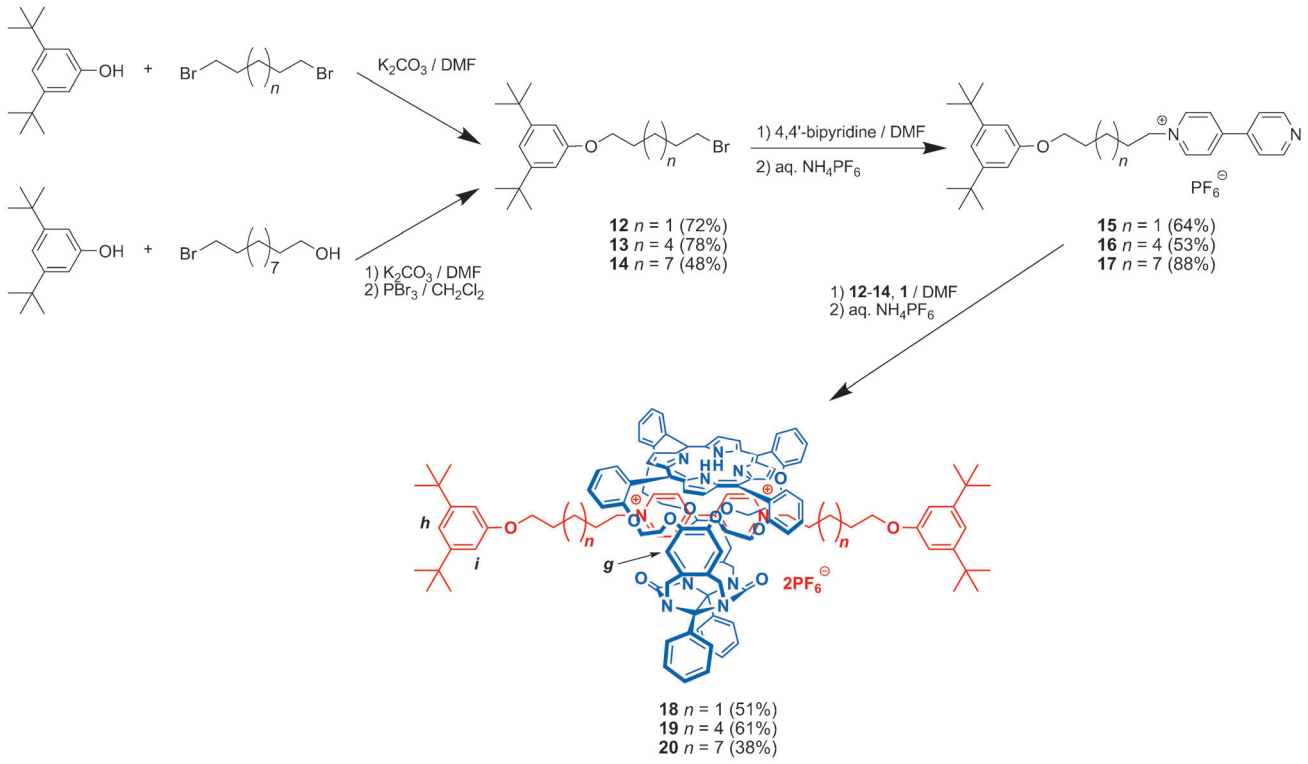

Scheme 5. Synthesis of [2]rotaxanes **18**–**20**.

stituents of **4** are too short to be engaged in an intramolecular crosslink. Hence, by varying the spacer length it is possible to control, at least to some extent, the outcome of the metathesis reaction.

Synthesis of [2]rotaxanes: It was decided to also synthesize a series of [2]rotaxanes based on **1**, containing threads of different lengths (Scheme 5), in order to be able to compare their physical properties with those of the aforementioned catenane structures. The synthesis of [2]rotaxanes **18**–**20** was based on our previously reported protocol.[9] It started with the synthesis of bulky alkyl bromides **12**–**14** by reacting the appropriate dibromides (in the case of **12** and **13**) with 3,5-di-*tert*-butylphenol under basic conditions in DMF. Compounds **12** and **13** were isolated in 70–80% yield. Bromide **14** was synthesized by first coupling 11-bromoundecan-1-ol and 3,5-di-*tert*-butylphenol (yield: 77%), after which the alcohol was converted into a bromide by reacting it with PBr_3 in CH_2Cl_2 to give **14** in 62% yield. This procedure was used because it was difficult to purify the product mixture obtained after reaction of the bulky phenol with 1,11-dibromoundecane. The bulky bromides were reacted with an excess of 4,4′-bipyridine in MeCN to give monoalkylated bipyridium derivatives **15**–**17** in yields up to 90%, after ion exchange using aqueous NH_4PF_6. It was now possible to synthesize the corresponding rotaxanes **18**–**20** by simply heating a mixture of **1**, five equivalents of **15**–**17**, respectively, and 40 equivalents of **12**–**14**, respectively, in DMF. After ion exchange with aqueous NH_4PF_6 and purification by column chromatography, the [2]rotaxanes were isolated in yields up to 60%.

Protonation-induced shuttling: With the novel interlocked porphyrins at hand, it was decided to investigate if these molecules could be used as molecular switches. We anticipated that protonation of the pyrrole nitrogen atoms of the porphyrin ring with trifluoroacetic acid (TFA) would result in an expulsion of the viologen moiety from the porphyrin cavity owing to Coulombic repulsion, as was observed previously in a related system reported by Gunter and Johnston.[15] Indeed, the addition of 5 vol% of TFA to a $CDCl_3$ solution of the simplest [2]catenane, **6**, thus providing protonated [2] catenane $[\mathbf{6}\cdot 2H]^{2+}$, resulted in dramatic downfield shifts for viologen resonances H_a ($\Delta\delta = +2.78$ ppm, see Scheme 2 for proton numbering) and H_b ($\Delta\delta = +3.77$ ppm), because of expulsion of the viologen from the cavity of **1** (Figure 3). In addition, a significant downfield shift was observed for alkene resonance H_c ($\Delta\delta = +0.53$ ppm). Both observations indicate a rotation of the viologen-containing ring with respect to the porphyrin host. Because the resonances of H_a, H_b, and H_c appear at positions where they are expected in noncatenated compounds, it can be concluded that the porphyrin bead in $[\mathbf{6}\cdot 2H]^{2+}$ does not reside on the viologen, whereas in **6**, it exclusively resides on this moiety. Detailed investigations using COSY and 2D-NOESY spectroscopy revealed that the protonated porphyrin in $[\mathbf{6}\cdot 2H]^{2+}$ is situated near one of the ether oxygen atoms of the thread, possibly because of the presence of $NH^+\cdots O$ hydrogen bonds, be-

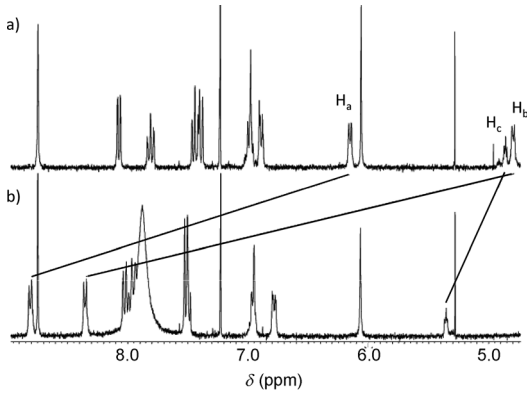

Figure 3. Part of the ^{1}H NMR spectra (300 MHz) of (a) unprotonated [2]catenane **6** and (b) protonated [2]catenane $[\mathbf{6}\cdot 2H]^{2+}$. See Scheme 2 and 3 for proton numbering.

cause increasingly larger upfield shifts are observed for the signals of H_d, H_e, and H_f (Table 1). The resonance for proton H_g in $[\mathbf{6}\cdot 2H]^{2+}$ could not be identified, as it was either obscured by other signals or severely broadened. The symmetry observed in the NMR spectrum of $[\mathbf{6}\cdot 2H]^{2+}$ can

Table 1. ^{1}H NMR data of [2]catenane **6** and protonated catenane $[\mathbf{6}\cdot 2H]^{2+}$.[a]

Proton	**6** (δ, ppm)	$[\mathbf{6}\cdot 2H]^{2+}$ (δ, ppm)	Shift (δ, ppm)
a	6.18	8.96	+2.78
b	4.80	8.57	+3.77
c	4.87	5.40	+0.53
d	1.20	0.63	−0.57
e	1.50	0.20	−1.30
f	1.68	−0.60	−2.28

[a] 500 MHz, 298 K, $CDCl_3$, ca. 10^{-3} M. See Scheme 2 and 3 for proton numbering.

be attributed to the porphyrin bead shuttling between two degenerate states in which the porphyrin is near the oxygen atoms in the viologen-containing ring.[16] To investigate this dynamic behavior further, variable-temperature ^{1}H NMR (VT-NMR) spectroscopy was carried out on $[\mathbf{6}\cdot 2H]^{2+}$. As is shown in Figure 4, lowering the temperature causes dramatic changes in the NMR spectrum. Notably, new resonances appear at high field (0 to −4 ppm), most probably as a result of shielding effects exerted by the porphyrin ring current on protons present inside the cavity. Low-temperature COSY experiments were used to assign some of these resonances, as is indicated for proton H_f. Not all signals could be assigned owing to the broadening of the spectra. However, it is clear from these experiments that protonation induces a motion in the [2]catenane, involving a switching of the porphyrin moiety between two degenerate states (Scheme 6). Using the coalescence method,[17] the rate and the corresponding activation Gibbs energy for this dynamic process were estimated to be $k_{278}=7.0\times10^3\ s^{-1}$ and $\Delta G^{\ddagger}_{278}=47\ kJ\,mol^{-1}$, respectively. It is, however, not known if, in this dynamic behavior, the shuttling between the two degenerate states takes place via the double bond, via the viologen moiety, or via both routes (Scheme 6).

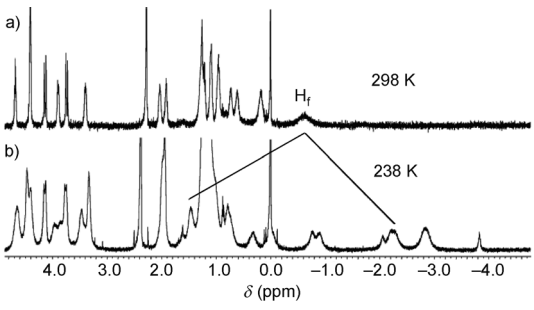

Figure 4. Parts of the ^{1}H NMR spectra (500 MHz) of $[\mathbf{6}\cdot 2H]^{2+}$ at (a) 298 K and (b) 238 K. See Scheme 3 for proton numbering.

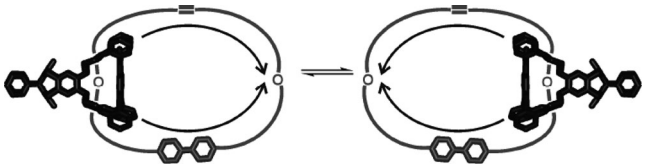

Scheme 6. Schematic representation of the proposed dynamic behavior in [2]catenane $[\mathbf{6}\cdot 2H]^{2+}$, demonstrating the possible pathways of movement of porphyrin host **1** along the thread between two degenerate states.

To obtain a better picture of the dynamic process, it was decided to investigate in more detail how a viologen can create a barrier for a shuttling process of the type shown above. To this end, the dynamic behavior of the series of [2]rotaxanes **18**–**20** as result of their protonation with TFA was investigated. In this type of interlocked molecule, similar dynamic behavior to that observed for the [2]catenane is only possible when the porphyrin overcomes the electrostatic barrier posed by the viologen. Protonating [2]rotaxane **18**, to give $[\mathbf{18}\cdot 2H]^{2+}$, again led to dramatic changes in the ^{1}H NMR spectra. Most strikingly, the signals of aromatic viologen protons H_a and H_b shifted downfield (by +1.69 ppm and +2.71 ppm, respectively). These resonances are, however, at a higher field (H_a at 7.81 ppm and H_b at 7.67 pm) than expected in a noncomplexed viologen. This is explained by assuming that the short C5-spacer and the blocking group prevent the viologen from completely leaving the porphyrin host, whereas the viologen can completely slide away from the porphyrin moiety in [2]catenane $[\mathbf{6}\cdot 2H]^{2+}$. Also, in the case of $[\mathbf{18}\cdot 2H]^{2+}$, a symmetrical NMR spectrum was observed, indicative of a movement of the porphyrin clip over the viologen moiety between the two blocking groups, a movement that is fast on the NMR time scale at room temperature. This dynamic behavior was confirmed by VT-NMR experiments (Figure 5), in which the temperature dependence of resonances H_g of the side wall of the porphyrin host and both resonances H_h and H_i of the blocking group are displayed.

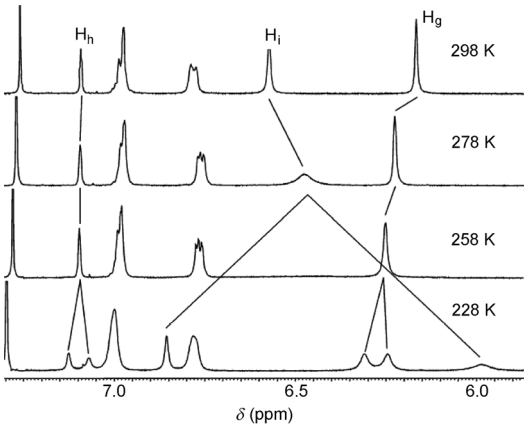

Figure 5. Parts of the VT-NMR spectra (500 MHz) of protonated [2]rotaxane [**18**·2H]$^{2+}$. See Scheme 5 for proton numbering.

As is shown in Figure 5, the signals H_h and H_i of the blocking group split up into a downfield- and an upfield-shifted signal, behavior that is a consequence of shielding effects of the porphyrin on the protons that are nearest to it. We propose that the porphyrin also reduces the conformational freedom of these protons because the upfield signals are somewhat broadened. Similar to what was observed in the VT-NMR study of the [2]catenane [**6**·2H]$^{2+}$, new resonances appeared below 0 ppm, resonances that are assigned to the aliphatic spacer protons that are situated inside the cavity (see below). It is therefore proposed that protonated [2]rotaxane [**18**·2H]$^{2+}$ shuttles between the two degenerate states that are created owing to the unfavorable electrostatic interactions between the doubly charged viologen moiety and the protonated porphyrin (Scheme 7).

The dynamic behavior of protonated rotaxanes [**19**·2H]$^{2+}$ and [**20**·2H]$^{2+}$ was also investigated by VT-NMR experiments. These complexes were found to display a similar dynamic motion; however, the increased spacer length between the viologen moiety and the blocking group had a remarkable effect on the Gibbs-energy barrier associated with the shuttling motion when compared to the shorter spaced rotaxane, [**18**·2H]$^{2+}$ (Table 2). This is most clearly exemplified in Figure 6, which shows the 0 to −4 ppm region of the ^{1}H NMR spectra of [**19**·2H]$^{2+}$ and [**20**·2H]$^{2+}$. At 298 K, the

Table 2. Thermodynamic and kinetic data for the shuttling process in protonated [2]rotaxanes [**18**–**20**·2H]$^{2+}$.

Rotaxane	Probe proton	T_c [K][a]	k_c [s^{-1}]	$\Delta G^{\ddagger}_c$ [kJ mol^{-1}][b]
[**18**·2H]$^{2+}$	i	258	970	48
[**19**·2H]$^{2+}$	a	244	62	51
[**20**·2H]$^{2+}$	g	302	71	63

[a] Coalescence temperature. [b] Estimated error 10 %. For proton numbering see Scheme 2 and 5.

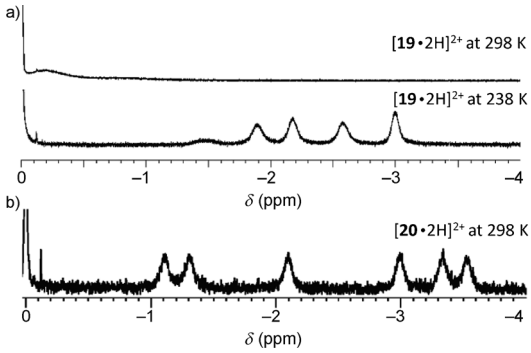

Figure 6. (a) Parts of the ^{1}H NMR spectra (500 MHz) of [2]rotaxane [**19**·2H]$^{2+}$ at 298 K and 238 K and (b) [2]rotaxane [**20**·2H]$^{2+}$ at 298 K, showing that at 298 K the shuttling equilibrium is fast on the NMR timescale for [**19**·2H]$^{2+}$ and slow for [**20**·2H]$^{2+}$.

shuttling between the two degenerate states in [**19**·2H]$^{2+}$ is fast on the NMR timescale, leading to a highly symmetrical spectrum that shows no resonances in this upfield region. If the temperature is lowered to 238 K, signals originating from the aliphatic spacer protons of the thread inside the cavity become visible between 0 and −4 ppm as a result of the fact that the exchange between the two degenerate states has now become slow on the NMR timescale. In marked contrast, the ^{1}H NMR spectrum of [**20**·2H]$^{2+}$ already shows similar signals in this region at 298 K, indicating that the Gibbs-energy barrier associated with the dynamic motion must be higher than that for the shorter-spaced rotaxanes. We therefore conclude that the Gibbs energy of activation for the shuttling process becomes higher as the spacer length increases. The thermodynamic parameters for the shuttling processes involving the [2]rotaxanes, [**18**–

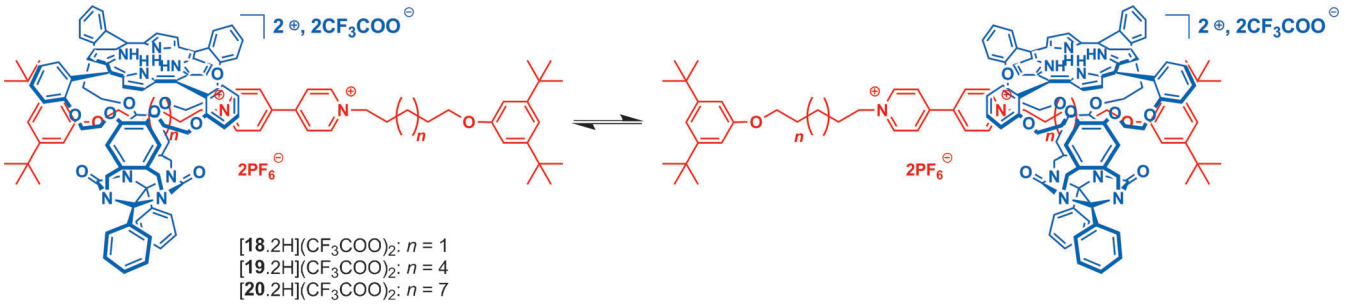

Scheme 7. Switching between two degenerate states in [2]rotaxanes [**18**–**20**·2H]$^{2+}$, as determined by VT-NMR experiments.

20·2H]$^{2+}$, as determined by the coalescence method, are summarized in Table 2. Notably, these values are not determined at the same temperature, so a detailed comparison between the $\Delta G^{\neq}_{c}$ values is not really allowed. Unfortunately, the activation parameters $\Delta H^{\neq}$ and $\Delta S^{\neq}$ could not be determined, as the quality of the spectra was not good enough for a line-shape analysis. However, we tentatively conclude that the energy barrier associated with the shuttling process increases as the spacer length increases. This can be explained by assuming that, in the case of a longer spacer, the doubly charged porphyrin host can slide away further from the doubly charged viologen moiety, thereby lowering the energies of the two degenerate states associated with the shuttling process because the electrostatic repulsion is reduced. Based on these observations, we propose that the porphyrin in [2]catenane [**6**·2H]$^{2+}$ shuttles between the two oxygen atoms and moves predominantly over the alkene part and not over the viologen, owing to unfavorable electrostatic interactions. This behavior is in marked contrast with the circumrotational movement of a similar [2]catenane, observed by Gunter and Johnston.[15] It is thus possible to induce a shuttling motion of the porphyrin host across the circular thread in [2]catenane **6** by simply protonating the porphyrin pyrrole nitrogen atoms. We also made attempts to investigate the dynamic behavior of the large catenanes, **10** and **11**. Unfortunately, complicated NMR spectra were observed in which the proton signals could not be assigned.

In a final series of experiments, we studied the photophysical properties of the interlocked complexes. We first studied [2]catenane [**6**·2H]$^{2+}$ by means of UV/Vis and fluorescence spectroscopy. Addition of an excess of TFA (5 vol%) to a $CHCl_3$ solution of [2]catenane **6** ([**6**] ~ 10^{-6} M) revealed a red shift of the Soret band from λ_{max} = 421 nm to λ_{max} = 437 nm, accompanied with significant broadening, which is a spectral change that is generally observed for protonation of simple porphyrins (Figure 7a). The fluorescence spectrum of **6** in $CHCl_3$ changed dramatically upon protonation of the porphyrin. Whereas in **6**, no detectable fluorescence emission could be observed upon excitation at λ_{max} = 421 nm, owing to efficient fluorescence quenching by the viologen inside the cavity, a large fluorescence emission peak at λ_{em} = 643 nm emerged upon addition of TFA and excitation at λ_{max} = 437 nm (Figure 7b).

Because, upon protonation of the porphyrin, the viologen moiety is expelled from the cavity, it can no longer act as a quencher, thus resulting in a dramatic increase in porphyrin fluorescence. The addition of pyridine to the solution resulted in deprotonation of [**6**·2H]$^{2+}$, regenerating **6**, as well as the previously observed UV/Vis and fluorescence spectra, indicating the reversible nature of the switching process. This result clearly demonstrates that [2]catenane **6** can be switched between a nonfluorescent and a fluorescent state by using simple acid–base chemistry.[18] The switching between the two states could be repeated at least 10 times without signs of fatigue, as was concluded from UV/Vis measurements. Rotaxanes **18**–**20** were also protonated and

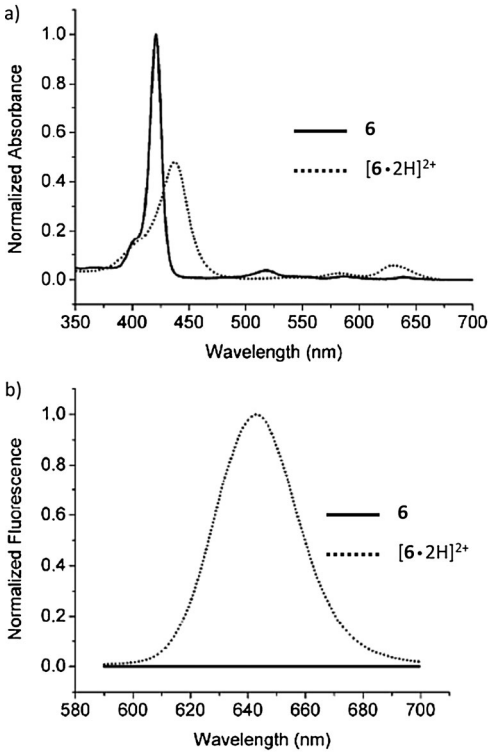

Figure 7. UV/Vis (a) and fluorescence (b) spectra of [2]catenanes **6** and [**6**·2H]$^{2+}$.

their fluorescence spectra recorded. Figure 8a shows the UV/Vis spectra of protonated catenane [**6**·2H]$^{2+}$ and protonated rotaxanes [**18**–**20**·2H]$^{2+}$. The protonated rotaxanes exhibit a broader Soret band than the one observed for the protonated catenane. This effect may be related to the different geometries of the two types of structures and the different types of interactions between the porphyrin and viologen moieties resulting from this. The fluorescence spectra display some interesting features (Figure 8b). Although [**18**–**20**·2H]$^{2+}$ display fluorescence emission upon excitation, the observed fluorescence intensities are much lower than the emission intensity originating from catenane [**6**·2H]$^{2+}$. Moreover, a clear spacer-length effect on the fluorescence intensity is observed: if the length of the rotaxane thread increases, the fluorescence emission also increases. This can be explained by assuming that when the distance between the viologen moiety and the porphyrin clip is larger, the viologen moiety is less efficient in quenching the fluorescence of the porphyrin.

Conclusion

We have demonstrated that catenanes based on porphyrin **1** and bis(olefin)-terminated viologens can be easily synthesized in high yields using an olefin-metathesis protocol. The size of the olefin substituents of the viologens has a marked effect on the products of the ring-closing reaction. Whereas a viologen with long substituents (21 atoms) yields a [2]cate-

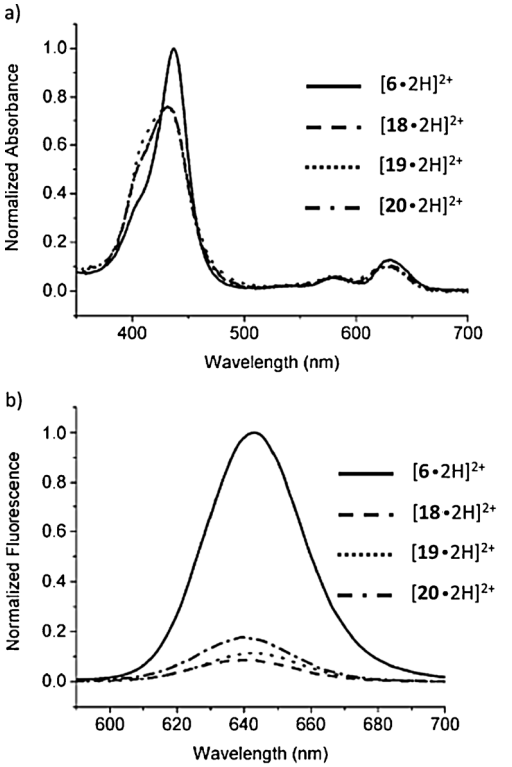

Figure 8. UV/Vis (a) and fluorescence (b) spectra of $[\mathbf{6}\cdot 2H]^{2+}$ and protonated rotaxanes $[\mathbf{18}–\mathbf{20}\cdot 2H]^{2+}$.

nane and a [3]catenane, the viologen with shorter substituents (8 atoms) gives a mixture of a [3]catenane, a [4]catenane, a [5]catenane, and higher oligomers, from which the [4]catenane and [5]catenane could be isolated. In addition, several [2]rotaxanes with threads of different lengths were successfully synthesized by S_N2-type reactions. The interlocked [2]catenane and [2]rotaxane structures show interesting switching behavior: a shuttling motion of the porphyrin in the described catenane and rotaxanes can be turned on and off using acid and base stimuli. The protonated porphyrin host in the [2]catenane shuttles between two oxygen atoms predominantly by a route via the carbon–carbon double bond in the aliphatic ring because the cationic viologen moiety poses a severe electrostatic barrier. In the case of the protonated [2]rotaxanes, the energy barrier associated with the shuttling is length dependent: when the spacer length between the viologen moiety and the blocking group of the thread is increased, the energy barrier also increases. The induction of motion of the porphyrin moiety in the [2]catenane and [2]rotaxanes is also accompanied by interesting photophysical changes. Upon protonation of the [2]catenane, the viologen that quenches the porphyrin fluorescence is expelled from the cavity, resulting in a dramatic increase in the fluorescence emission. Similar effects were observed for the [2]rotaxanes, but not as dramatic as in the case of the [2]catenane, and a clear dependency of the fluorescence properties on the length of the space between the viologen and the blocking group was observed.

Following the protocols described in this paper, we are currently planning the synthesis of functional catenane structures derived from metal–porphyrin (metal is Zn or Mn) glycoluril compounds. These will be allowed to form double-cage compounds with other glycoluril derivatives as schematically shown in Figure 1. The study of the properties of these systems as a first step towards a molecular device in which information can be transferred is envisaged.

Experimental Section

Materials and methods: Tetrahydrofuran was distilled under nitrogen from sodium and benzophenone. Acetonitrile was distilled under nitrogen from calcium hydride. Chloroform was distilled under nitrogen from calcium chloride. *n*-Hexane was distilled under nitrogen from sodium. Dimethylformamide was dried over BaO for one week and then vacuum distilled. The first 30% of the distillate was discarded. All other solvents and chemicals were commercially available and used without further purification. Compounds **12** and **15** were synthesized as described previously.[9] BioRad Biobeads (SX-1) were used for size-exclusion chromatography. Silica 60 (Merck) was used for column chromatography. Fluorescence experiments were performed on a Perkin–Elmer LS50B luminescence spectrometer equipped with a thermostatted cuvette holder. UV/Vis spectra were recorded on a Varian Cary 50 Conc spectrometer. ^{1}H NMR and ^{13}C NMR spectra were recorded on a Bruker DPX-200, AM-300, or Bruker DRX-500 spectrometers. Chemical shifts are reported in ppm downfield from internal tetramethylsilane (0.00 ppm) in the case of ^{1}H NMR and ^{13}C NMR spectra in $CDCl_3$ or $CDCl_3/CD_3CN$ (1:1, *v*/*v*), otherwise the solvent peak was used as a reference (CD_3CN: 1.94 ppm). MALDI-TOF spectra were recorded on a Bruker Biflex III spectrometer using dithranol as a matrix.

Synthetic procedures and compound data

10-(10-Bromodecyloxy)dec-1-ene (2): Under an argon atmosphere, dec-9-en-1-ol (1.4 g, 9 mmol) was added to a mixture of NaH (384 mg, 9.6 mmol, 60% dispersion in mineral oil) in argon-purged THF (15 mL). After the evolution of hydrogen gas had ceased, 1,10-dibromodecane (16.1 g, 53.6 mmol) was added and the resulting mixture was stirred for 5 days. The solvent was removed by rotary evaporation, after which the resulting crude product was dissolved in Et_2O. This solution was washed with water, dried ($MgSO_4$), filtered, and evaporated to dryness. The residue was purified by column chromatography (silica, *n*-heptane, $R_f = 0.65$) to yield **2** as a clear, colorless oil (1.5 g, 44%). ^{1}H NMR ($CDCl_3$, 200 MHz) $\delta = 5.90$–5.70 (m, 1H; $H_2C{=}CH$), 5.03–4.88 (m, 2H; $H_2C{=}CH$), 3.45–3.33 (m, 6H; CH_2OCH_2, CH_2Br), 2.04 (q, $^3J(H,H) = 7.0$ Hz, 2H; $H_2C{=}CHCH_2$), 1.69–1.20 ppm (m, 28H; CH_2); ^{13}C NMR ($CDCl_3$, 125 MHz) $\delta = 139.2$, 114.2, 71.1, 37.2, 33.8, 298, 29.5, 28.9, 26.3 ppm.

(*N*,*N*′)-Di-(1-(10-(dec-9-enyloxy)decyl)-4,4′-bipyridinium dihexafluorophosphate (3): A mixture of 4,4′-bipyridine (102 mg, 0.65 mmol) and **2** (1.23 g, 3.3 mmol) in DMF (1 mL) was stirred overnight under a N_2 atmosphere at 100 °C. After cooling, Et_2O was added and the resulting precipitate was filtered and washed with Et_2O and MeCN. The solid was dissolved in $MeCN/H_2O$ (1:1, *v*/*v*) after which the addition of a saturated solution of NH_4PF_6 in H_2O resulted in the precipitation of **3**. The solid was recrystallized from hot MeOH and washed with MeOH and Et_2O to give **3** as a white solid (153 mg, 23%). M.p. 255 °C (decomposed); ^{1}H NMR ($CDCl_3/CD_3CN$ (1:1, *v*/*v*), 200 MHz) $\delta = 8.90$ (d, $^3J(H,H) = 7.0$ Hz, 4H; BipyH,), 8.40 (d, $^3J(H,H) = 7.0$ Hz, 4H; BipyH), 5.93–5.70 (m, 2H; $H_2C{=}CH$), 5.05–4.86 (m, 4H; $H_2C{=}CH$), 4.61 (t, $^3J(H,H) = 6.4$ Hz, 4H; $BipyCH_2$), 3.36 (t, $^3J(H,H) = 6.4$ Hz, 8H; CH_2O), 2.02 (q, $^3J(H,H) = 7.0$ Hz, 4H; $H_2C{=}CHCH_2$), 1.60–1.20 ppm (m, 56H; CH_2); ^{13}C NMR ($CDCl_3$, 125 MHz) $\delta = 147.1$, 144.1, 138.7, 126.5, 113.2, 69.9, 32.9, 30.4, 29.0, 28.6, 28.0, 25.3 ppm. IR (KBr) $\tilde{\nu} = 2926$, 2854,1647, 1508, 1472, 1379, 1182, 1124, 836, 558 cm^{-1}; MS (MALDI-TOF): *m*/*z*: 746 $[M-2PF_6]^+$; HRMS (ESI-TOF): *m*/*z* calcd for $C_{50}H_{86}F_6N_2O_2P$: 891.63311

$[M-PF_6]^+$; found: 891.63096; *m/z* calcd for $C_{50}H_{86}N_2O_2$: 746.66674 $[M-2PF_6]^+$; found: 746.66893.

(*N,N*′)-Di-(1-(oct-7-enyl))-4,4′-bipyridinium dihexafluorophosphate (4): A mixture of 4,4′-bipyridine (100 mg, 0.64 mmol) and 8-bromo-octene (1.2 g, 6.3 mmol) in DMF (1 mL) was stirred overnight under a N_2 atmosphere at 100 °C. After cooling, Et_2O was added and the resulting precipitate was filtered and washed with Et_2O and MeCN. The solid was dissolved in MeCN and a saturated solution of NH_4PF_6 in H_2O was added, which resulted in the precipitation of **4** as a white solid in a yield of 260 mg (61 %). M.p. 249 °C (decomposed); ^{1}H NMR (CD_3CN, 200 MHz) δ = 8.91 (d, ^3J(H,H) = 6.9 Hz, 4H; BipyH), 8.39 (d, ^3J(H,H) = 6.9 Hz, 4H; BipyH), 5.95–5.73 (m, 2H; H_2C=C*H*), 5.11–4.89 (m, 4H; *H*$_2$C=CH), 4.61 (t, ^3J(H,H) = 7.4 Hz, 4H; BipyCH_2), 2.08 (m, 8H; CH_2), 1.39 ppm (bs, 12H; CH_2); ^{13}C NMR ($CDCl_3$, 125 MHz) δ = 149.0, 144.7, 137.9, 126.4, 113.4, 61.4, 32.5, 30.1, 27.5, 27.3, 24.6 ppm; IR (KBr) $\tilde{\nu}$ = 3149, 3084, 2933, 2862, 1647, 1565, 1512, 1457, 1230, 1179, 836, 558 cm^{-1}; MS (MALDI-TOF): *m/z*: 378 $[M-2PF_6]^+$; HRMS (ESI-TOF): *m/z* calcd for $C_{26}H_{38}F_6N_2P$: 523.26768 $[M-PF_6]^+$; found: 523.26734.

[2]Catenane 6 and [3]catenane 7: A solution of **1** (40 mg, 0.03 mmol) in a minimal amount of $CHCl_3$ and a solution of **3** (30.8 mg, 0.03 mmol) in a minimal amount of acetone were mixed, and the solvent was evaporated. The resulting solid was dissolved in a minimal amount of CH_2Cl_2 and precipitated in *n*-hexane. After drying in vacuo, the thus obtained [2]pseudorotaxane **5** was dissolved in CH_2Cl_2 (60 mL), and the first generation Grubbs' catalyst (5 mg, 6.1 μmol) was added under an argon atmosphere. The resulting mixture was stirred overnight at room temperature, after which the solvent was removed by rotary evaporation. The crude mixture was subjected to column chromatography (silica, CH_2Cl_2/$MeNO_2$/MeOH, 8:1:1, *v/v/v*) yielding a mixture of **1**, **6**, and **7**. These compounds were separated by column chromatography (first column: biobeads, CH_2Cl_2; second column: silica, 3 % MeOH/CH_2Cl_2, *v/v*) to yield **6** (48 mg, 69 %, R_f = 0.26) and **7** (2 mg, 3 %, R_f = 0.14) as purple solids.

Data for **5**: ^{1}H NMR ($CDCl_3$, 500 MHz, for proton numbering see figure below and Scheme 1 and 2): δ = 9.06 and 8.77 (2 s, 8H; H12–13), 8.09 (d, ^3J(H,H) = 6.9 Hz, 4H; H11), 7.82 (bt, ^3J(H,H) = 7.8 Hz, 4H; H10), 7.45 (t, ^3J(H,H) = 7.0 Hz, 4H; H9), 7.40 (d, ^3J(H,H) = 7.0 Hz, 4H; H8), 7.2–6.7 (m, 10H; H1–3), 6.12 (d, ^3J(H,H) = 5.5 Hz, 4H; Hb), 6.05 (s, 4H; H5), 5.85–5.75 (m, 2H; H_2C=C*H*), 5.05–4.85 (m, 4H; *H*$_2$C=CH), 4.84 (b, 4H; Ha), 4.32 (m, 4H; H7), 4.26 (d, ^2J(H,H) = 15.6 Hz, 4H; H4), 4.03 (m, 4H, H7), 3.72 (d, ^2J(H,H) = 15.6 Hz, 4H; H4), 3.5–3.4 (m, 16H; Hc, Hl, Hm, H6), 3.33 (m, 4H; Hc), 2.76 (m, 4H; H6), 2.04 (m, 4H; CH_2), 1.7–1.55 (m, 8H; CH_2), 1.5–1.15 (m, 34H; CH_2), 1.08 (m, 8H; CH_2), 0.90 (m, 8H; CH_2), −2.83 ppm (s, 2H; H14).

Data for **6**: M.p. > 300 °C (decomposed); ^{1}H NMR ($CDCl_3$, 500 MHz, for proton numbering see figure below and Scheme 1 and 2): δ = 9.08 (s, 4H; H12), 8.79 (s, 4H; H13), 8.11 (dd, ^3J(H,H) = 7.3 Hz, ^5J(H,H) = 1.5 Hz, 4H; H11), 7.84 (dt, ^3J(H,H) = 8.0 Hz, ^5J(H,H) = 1.6 Hz, 4H; H10), 7.47 (t, ^3J(H,H) = 7.5 Hz, 4H; H9), 7.42 (d, ^3J(H,H) = 8.4 Hz, 4H; H8), 7.05–6.97 (m, 6H; H1,2), 6.95–6.90 (m, 4H; H3), 6.18 (d, ^3J(H,H) = 4.8 Hz, 4H; Hb), 6.08 (s, 4H; H5), 4.93 (m; Hu, *cis*), 4.87 (m; Hu, *trans*), 4.79 (d, ^3J-(H,H) = 4.4 Hz, 4H; Ha), 4.35 (m, 4H; H7), 4.28 (d, ^2J(H,H) = 16.0 Hz, 4H; H4), 4.04 (m, 4H; H7), 3.74 (d, ^2J(H,H) = 15.8 Hz, 4H; H4), 3.52 (m, 4H; H6), 3.48 (m, 8H; Hl, Hm), 3.44 (m, 4H; Hc), 2.78 (m, 4H; H6), 1.67 (m, 8H; Hk, Hn), 1.60 (m; Ht, *cis*), 1.50 (m, 8H; Ho, Hj), 1.46 (m; Ht, *trans*), 1.30 (m; 8H, He, Hf), 1.20 (m, 8H; Hi, Hp), 1.08 (m, 8H; Hh, Hq), 0.96 (m, 8H; Hg, Hr), 0.92 (m; Hs, *cis*), 0.87 (m; Hs, *trans*), −2.81 ppm (s, 2H; H14); ^{13}C NMR ($CDCl_3$, 125 MHz) δ = 158.6, 158.1, 146.2, 142.5, 135.6, 131.2, 130.7, 130.1, 129.8, 129.0, 128.7, 128.1, 123.3, 120.5, 116.7, 116.4, 85.4, 70.9, 68.5, 67.4, 44.0, 32.3, 30.9, 30.5, 29.9, 29.6, 29.4, 29.1, 28.8, 27.0, 26.3, 26.1 ppm. IR (KBr) $\tilde{\nu}$ = 3060, 2928, 2854, 1696, 1653, 1635, 1598, 1581, 1560, 1517, 1465, 1448, 1428, 1384, 1347, 1283, 1251, 1214, 1120, 1064, 967, 956, 841, 805, 752, 720, 696, 668, 557 cm^{-1}; MS (MALDI-TOF): *m/z* 2063.1 $[M-2PF_6]^+$, 2208.1 $[M-PF_6]^+$.

Data for **7**: M.p. > 300 °C (decomposed); ^{1}H NMR ($CDCl_3$, 500 MHz, for proton numbering see figure below and Scheme 1 and 2): δ = 9.02 (s, 8H; H12), 8.65 (s, 8H; H13), 8.02 (dd, ^3J(H,H) = 7.3 Hz, ^5J(H,H) = 1.7 Hz, 8H; H11), 7.81 (dt, ^3J(H,H) = 8.0 Hz, ^5J(H,H) = 1.5 Hz, 8H; H10), 7.45–7.35 (m, 16H; H9, H10), 7.10–6.90 (m, 20H; H1–3), 6.05 (bs, 8H; Hb), 5.88 (bs, 8H; H5), 5.44–5.35 (m, 4H; Hu), 4.62 (bs, 8H; Ha), 4.30–4.21 (m, 8H; H7), 4.16 (d, ^2J(H,H) = 15.9 Hz, 8H; H4), 3.88–3.75 (m, 8H; H7), 3.60 (d, ^2J(H,H) = 16.0 Hz, 8H; H4), 3.52–3.43 (m, 16H; Hl, Hm), 3.40–3.20 (m, 16H; Hc, H6), 2.66–2.55 (m, 8H; H6), 2.10–0.70 (m; CH_2), −2.95 ppm (s, 4H; H14); MS (MALDI-TOF): *m/z* 4125.6, 4271.6, 4416.4, 4560.7 $[M-nPF_6]^+$ (*n* = 1–4).

[4]Catenane 10 and [5]catenane 11: A solution of **1** (45.6 mg, 0.034

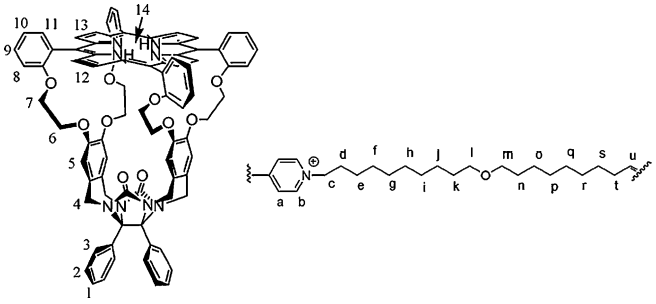

mmol) in a minimal amount of $CHCl_3$ and a solution of **4** (20.7 mg, 0.031 mmol) in a minimal amount of acetone were mixed, and the solvent was evaporated. The resulting solid was dissolved in a minimal amount of CH_2Cl_2 and precipitated in *n*-hexane. After drying in vacuo, the thus obtained [2]pseudorotaxane **8** was dissolved in CH_2Cl_2 (34 mL), 2 mg of first generation Grubbs' catalyst was added, and the resulting solution was refluxed under an argon atmosphere. After 30 min., another 2 mg of Grubbs' catalyst was added and refluxing was continued for 6 hrs after which a last portion of 0.5 mg Grubbs' catalyst was added (total added catalyst: 4.5 mg, 5.5 μmol). After an additional hour of refluxing, the solution was allowed to cool and a drop of ethylvinyl ether was added after which the solvent was evaporated. The crude mixture was subjected to column chromatography (silica, CH_2Cl_2/$MeNO_2$/MeOH, 8:1:1, *v/v/v*) yielding a mixture of **1**, **9**, **10**, **11**, and higher oligomers. This mixture was subjected to size-exclusion chromatography (biobeads, CH_2Cl_2) from which the [4]catenane **10** and the [5]catenane **11** could be isolated. Both compounds were subjected to another size-exclusion column to give **10** (12 mg, 18 %) and **11** (7 mg, 11 %) as purple solids. M.p. > 300 °C (decomposed); the ^{1}H NMR spectra were assigned based on 2D-COSY and 2D-NOESY spectra, therefore, some values for the integrals and signal shapes are not given.

Data for **10**: ^{1}H NMR ($CDCl_3$, 500 MHz) δ = 9.07 (m, 12H; H12), 8.72 (m, 12H; H13), 8.06 (m, 12H; H11), 7.82 (m, 12H; H10), 7.44 (m, 24H; H8, H9), 7.1–6.6 (m, 30H; H1–3), 6.54 (bs; BipyH), 6.42 (bs; BipyH), 6.2–5.8 (m; BipyH), 6.05–5.9 (m; H5), 5.57 (bs; CH=CH, *trans*), 5.49 (bs; CH=CH, *cis*), 4.84 (bs; BipyH), 4.74 (bs; BipyH), 4.60 (bs; BipyH), 4.53 (bs; BipyH), 4.40 (bs; BipyH), 4.29 (bs; H7), 4.19 (d, ^2J(H,H) = 15.8 Hz; H4), 4.05–3.8 (m; H7), 3.65–3.05 (m; BipyCH_2), 3.45–3.30 (m; H6), 2.80–2.40 (m; H6), 2.15 (bs; CH_2CH=, *cis*), 2.08 (bs; CH_2CH=, *trans*), 1.60–0.7 (m; CH_2), −2.80–−3.0 ppm (m, 6H; H14); ^{13}C NMR ($CDCl_3$, 125 MHz) δ = 158.4, 146.0, 142.5, 135.7, 130.6, 130.1, 128.7, 128.0, 120.3, 116.4, 112.4, 85.3, 68.2, 67.2, 64.4, 43.9, 33.9, 30.9, 29.8, 28.8, 25.9, 25.1 ppm. MS (MALDI-TOF): *m/z* 5088, 5225, 5370, 5516, 5661, 5805 $[M-nPF_6]^+$ (*n* = 1–6).

Data for **11**: ^{1}H NMR ($CDCl_3$, 500 MHz, see figure above for proton numbering) δ = 9.07 (app. d, 16H; H12), 8.77 (bs, 16H; H13), 8.07 (bs, 16H; H11), 7.83 (bm, 16H; H10), 7.45 (bm, 32H; H8, H9), 7.10–6.65 (m, 40H; H1–3), 6.38 (bs; BipyH), 6.22 (bs; BipyH), 6.19 (bs; BipyH), 6.02 (bs; H5) 6.00 (bs; BipyH), 5.54 (bs; CH=CH, *trans*), 5.49 (bs; CH=CH, *cis*), 4.69 (bs; BipyH), 4.65 (bs; BipyH), 4.57 (bs; BipyH), 4.48 (bs; BipyH), 4.35 (bs; H7), 4.20 (m; H4), 4.02 (bs; H7), 3.56 (m; H4), 3.50–3.25 (m; BipyCH_2), 3.45 (bs; H6), 2.75 (bs; H6), 2.16 (bs; CH_2CH=, *cis*), 2.09 (bs; CH_2CH=, trans), 1.70–0.80 (m; CH_2), −2.87 ppm (s, 8H; H14); ^{13}C NMR ($CDCl_3$, 125 MHz) δ = 158.7, 148.7, 146.2, 142.7, 139.8, 135.6, 132.9, 130.6, 130.1, 128.6, 128.0, 123.3, 120.4, 116.4, 112.4, 85.3, 68.6, 67.5, 64.5, 44.1, 34.4, 33.3, 32.3, 31.9, 30.9, 29.7, 29.6, 29.3, 29.1, 28.6, 25.9,

25.0 ppm; MS (MALDI-TOF): *m/z* 6778, 6923, 7068, 7213, 7358, 7503, 7648, 7793 $[M-nPF_6]^+$ ($n=1$–8).

1-(8-Bromooctyloxy)-3,5-di-*tert*-butylbenzene (13): A mixture of 3,5-di-*tert*-butylphenol (3 g, 14.5 mmol), 1,8-dibromooctane (20 g, 73.5 mmol) and K_2CO_3 (10 g, 72.4 mmol) in DMF (30 mL) was stirred overnight under an argon atmosphere, after which the solvent and the remaining 1,8-dibromooctane was distilled off. The resulting crude product was subjected to column chromatography (silica, *n*-heptane, $R_f=0.08$) to yield **13** as a colorless oil (4.5 g, 78%). ^{1}H NMR ($CDCl_3$, 200 MHz) $\delta=7.01$ (t, ^4J(H,H) = 1.7 Hz, 1H; *para*-ArH), 6.75 (d, ^4J(H,H) = 1.7 Hz, 2H; *ortho*-ArH), 3.96 (t, ^3J(H,H) = 6.4 Hz, 2H; OCH_2), 3.39 (t, ^3J(H,H) = 6.9 Hz, 2H; CH_2Br), 1.95–1.72 (m, 4H; CH_2), 1.57–1.23 (m, 8H; CH_2), 1.31 ppm (s, 18H; CCH_3); ^{13}C NMR ($CDCl_3$, 125 MHz) $\delta=158.6$, 152.1, 114.8, 108.8, 67.6, 35.0, 34.0, 32.8, 31.4, 29.4, 29.2, 28.7, 28.1, 26.0 ppm; IR (KBr) $\tilde{\nu}=2964$, 2861, 1593, 1478, 1465, 1429, 1393, 1362, 1324, 1300, 1247, 1219, 1204, 1122, 1059, 937, 900, 863, 845, 707, 668, 645, 564 cm^{-1}; MS (GC-MS): *m/z* 396 $[M^+]$; HRMS (EI-TOF): *m/z* calcd for $C_{22}H_{37}BrO$: 396.20278 $[M^+]$; found: 396.20190.

11-(3,5-Di-*tert*-butyl-phenoxy)-undecan-1-ol: 3,5-Di-*tert*-butylphenol (300 mg, 1.46 mmol) and 11-bromoundecanol (350 mg, 1.39 mmol) were suspended in argon-flushed DMF (10 mL). K_2CO_3 (750 mg, 5.43 mmol) was added and the mixture was heated overnight at 100 °C under argon. After cooling, the solvent was evaporated and the residue dissolved in CH_2Cl_2. The organic layer was washed first with aqueous 1 N HCl and then with an aqueous saturated $NaHCO_3$ solution. After evaporation of the solvent, the crude product was purified by column chromatography (Silica 60H, 5% EtOAc/*n*-heptane, *v/v*, $R_f=0.05$) to give the desired product as a colorless oil (420 mg, 77%). ^{1}H NMR ($CDCl_3$, 300 MHz) $\delta=6.98$ (t, ^4J(H,H) = 1.8 Hz, 1H; ArH), 6.73 (d, ^4J(H,H) = 1.8 Hz, 2H; ArH), 3.94 (t, ^3J(H,H) = 6.6 Hz, 2H; $ArOCH_2$), 3.63 (m, 2H; CH_2OH), 1.78 (m, 2H; CH_2CH_2OH), 1.7–1.1 (m, 17H; CH_2 and OH), 1.31 ppm (s, 18H; CH_3); ^{13}C NMR ($CDCl_3$, 125 MHz) $\delta=158.7$, 152.1, 114.8, 108.8, 67.7, 63.1, 35.0, 32.8, 31.4, 29.6, 26.5, 29.4, 26.1, 25.7 ppm; IR (KBr) $\tilde{\nu}=$ 3373, 3076, 928, 2856, 1592, 1478, 1465, 1429, 1393, 1362, 1324, 1300, 1247, 1219, 1204, 1122, 1058, 938, 901, 862, 844, 707, 636 cm^{-1}; MS (MALDI-TOF): *m/z* 377 $[M+H]^+$.

1-(11-Bromoundecyloxy)-3,5-di-*tert*-butylbenzene (14): 11-(3,5-Di-*tert*-butylphenoxy)-undecan-1-ol (420 mg, 1.12 mmol) was dissolved in freshly distilled $CHCl_3$ (15 mL) under argon and this solution was cooled to 0 °C. PBr_3 (0.5 g, 1.85 mmol) was added and the mixture was allowed to warm to room temperature and stirred overnight. Water was added dropwise to quench the reaction, and the mixture was extracted with aqueous 0.5 N NaOH. The organic layer was evaporated to dryness, and the residue was purified by column chromatography (Silica 60H, $CHCl_3$, $R_f=0.95$) to give **14** (305 mg, 62%) as a colorless oil. ^{1}H NMR ($CDCl_3$, 300 MHz) $\delta=$ 6.98 (t, ^4J(H,H) = 1.8 Hz, 1H; ArH), 6.72 (d, ^4J(H,H) = 1.8 Hz, 2H; ArH), 3.94 (t, ^3J(H,H) = 6.6 Hz, 2H; $ArOCH_2$), 3.39 (t, ^3J(H,H) = 6.5 Hz, 2H; CH_2Br), 1.80 (m, 4H; CH_2), 1.6–1.2 (m, 16H; CH_2), 1.31 ppm (s, 18H; CH_3); ^{13}C NMR ($CDCl_3$, 125 MHz) $\delta=158.9$, 152.1, 114.8, 108.9, 67.7, 35.0, 34.1, 32.8, 31.5, 29.5, 29.4, 28.8, 28.2, 26.1 ppm; IR (KBr) $\tilde{\nu}=$ 3076, 2964, 2868, 1593, 1479, 1429, 1393, 1362, 1323, 1300, 1247, 1218, 1204, 1122, 1060, 1008, 939, 900, 863, 845, 814, 736, 707, 643, 563 cm^{-1}; MS (GC-MS): *m/z* 440 $[M+H]^+$; HRMS (EI-TOF): *m/z* calcd for $C_{25}H_{43}BrO$: 438.24973 $[M^+]$; found: 438.24955.

1-(8-(3,5-Di-*tert*-butylphenoxy)octyl)-4,4′-bipyridin-1-ium hexafluorophosphate (16): 4,4′-Bipyridine (4 g, 25.6 mmol) and **13** (1 g, 2.5 mmol) were dissolved in MeCN (25 mL). The solution was refluxed overnight. After cooling Et_2O was added and the resulting precipitate was filtered off and washed with Et_2O. The resulting gum was dissolved in hot water and a saturated aqueous solution of NH_4PF_6 was added resulting in the formation of an oil which solidified into a white solid upon scratching the inside of the flask. Filtration gave **16** as a white powder (820 mg, 53%). M.p. 116 °C (decomposed); ^{1}H NMR (CD_3CN, 200 MHz) $\delta=8.88$ (bs, 2H; BipyH), 8.89 (d, ^3J(H,H) = 7.1 Hz, 2H; BipyH), 8.32 (d, ^3J(H,H) = 6.6 Hz, 2H; BipyH), 7.93 (d, ^3J(H,H) = 5.9 Hz, 2H; BipyH), 7.03 (t, ^4J(H,H) = 1.7 Hz, 1H; *para*-ArH), 6.72 (t, ^4J(H,H) = 1.7 Hz, 2H; *ortho*-ArH), 4.56 (t, ^3J(H,H) = 7.3 Hz, 2H; $BipyCH_2$), 3.97 (t, ^3J(H,H) = 6.4 Hz, 2H; OCH_2), 2.01 (q, ^3J(H,H) = 6.6 Hz, 2H; CH_2), 1.74 (q, ^3J(H,H) = 6.6 Hz, 2H; CH_2), 1.40 (bs, 8H; CH_2), 1.28 ppm (s, 18H; CCH_3); ^{13}C NMR ($CDCl_3$, 125 MHz) $\delta=158.6$, 154.4, 152.2, 151.4, 144.7, 140.9, 126.0, 121.4, 114.8, 108.8, 67.5, 62.2, 35.0, 31.4, 31.3, 29.4, 29.0, 28.8, 25.9 ppm; IR (KBr) $\tilde{\nu}=3136$, 2955, 2870, 1646, 1594, 1550, 1527, 1459, 1430, 1413, 1362, 1324, 1302, 1248, 1222, 1174, 112, 1063, 833, 557 cm^{-1}; MS (MALDI-TOF): *m/z* 474 $[M-PF_6+H]^+$; HRMS (ESI-TOF): *m/z* calcd for $C_{32}H_{45}N_2O$: 473.35319 $[M-PF_6]^+$; found: 473.35415.

1-(11-(3,5-Di-*tert*-butylphenoxy)undecyl)-4,4′-bipyridin-1-ium hexafluorophosphate (17): Compound **14** (85 mg, 0.19 mmol) and 4,4-bipyridine (300 mg, 1.9 mmol) were dissolved in acetonitrile (10 mL). The mixture was refluxed overnight under argon. After cooling, the solvent was evaporated and the residue was dissolved in $CHCl_3$ (5 mL). An aqueous saturated NH_4PF_6 solution (5 mL) was added, and the mixture was stirred vigorously for 2 h. The organic layer was separated, washed with water and evaporated to dryness. The crude product was purified by column chromatography (Silica 60H, 3% MeOH/$CHCl_3$, *v/v*, $R_f=0.02$) to give **17** (112 mg, 88%) as a yellowish oil/wax. ^{1}H NMR ($CDCl_3$, 300 MHz) $\delta=8.81$ (d, ^3J(H,H) = 6.0 Hz, 2H; BipyH), 8.70 (d, ^3J(H,H) = 5.1 Hz, 2H; BipyH), 8.13 (d, ^3J(H,H) = 6.9 Hz, 2H; BipyH), 7.58 (d, ^3J(H,H) = 4.5 Hz, 2H; BipyH), 6.95 (t, ^4J(H,H) = 1.8 Hz, 1H; ArH), 6.70 (d, ^4J(H,H) = 1.8 Hz, 2H; ArH), 4.55 (t, ^3J(H,H) = 7.2 Hz, 2H; CH_2N), 3.91 (t, 2H; $ArOCH_2$), 1.98 (m, 2H; CH_2), 1.74 (m, 2H; CH_2), 1.6–1.1 (m, 16H; CH_2), 1.28 ppm (s, 18H; CH_3); ^{13}C NMR ($CDCl_3$, 125 MHz) $\delta=15.7$, 154.4, 152.1, 151.4, 144.7, 140.9, 126.0, 121.4, 114.8, 108.8, 67.7, 62.3, 35.0, 31.4, 26.1, 26.0, 25.9 ppm; IR (KBr) $\tilde{\nu}=2958$, 2927, 2856, 1793, 1735, 1648, 1595, 1546, 1526, 1465, 1430, 1412, 1393, 1363, 1334, 1301, 1247, 1220, 1204, 1184, 1122, 1060, 860, 834, 815, 724, 708, 669, 558 cm^{-1}; MS (MALDI-TOF): *m/z* 516 $[M-PF_6+H]^+$; HRMS (ESI-TOF): *m/z* calcd for $C_{35}H_{51}N_2O$: 515.40014 $[M-PF_6]^+$; found: 515.40100.

[2]Rotaxane 18: Porphyrin **1** (10 mg, 7.4 μmol), pyridinium salt **15** (21 mg, 37 μmol), and bromide **12** (104 mg, 293 μmol) were dissolved in DMF (1.5 mL). The resulting solution was stirred overnight at 90 °C under an argon atmosphere. After cooling, the solvent was evaporated and the resulting solid was dissolved in MeCN. To this solution a saturated aqueous solution of NH_4PF_6 was added. Water and $CHCl_3$ were added and the organic layer was separated and evaporated to dryness. The crude mixture was subjected to column chromatography (silica, CH_2Cl_2 to 0.3% MeOH/CH_2Cl_2 (*v/v*) to 0.5% MeOH/CH_2Cl_2, *v/v*) to yield **18** as a purple solid (9 mg, 51%). M.p. > 300 °C (decomposed); ^{1}H NMR ($CDCl_3$, 500 MHz) $\delta=9.11$ (s, 4H; H12), 8.78 (s, 4H; H13), 8.09 (dd, ^3J(H,H) = 7.4 Hz, ^5J(H,H) = 1.7 Hz, 4H; H11), 7.80 (dt, ^3J(H,H) = 8.0 Hz, ^5J(H,H) = 1.7 Hz, 4H; H10), 7.44 (t, ^3J(H,H) = 7.4 Hz, 4H; H9), 7.40 (d, ^3J(H,H) = 8.5 Hz, 4H; H8), 7.06 (t, ^5J(H,H) = 1.5 Hz, 2H; *para*-ArH (thread)), 7.05–6.96 (m, 6H; H1, H2), 6.92–6.88 (m, 4H; H3), 6.83 (d, ^5J(H,H) = 1.6 Hz, 4H; *ortho*-ArH (thread)), 6.15 (bd, ^3J(H,H) = 5.2 Hz, 4H; BipyH), 6.07 (s, 4H; H5), 4.96 (bs, 4H; BipyH), 4.35 (m, 4H; H7), 4.23 (d, ^2J(H,H) = 15.9 Hz, 4H; H4), 4.02 (m, 4H; H7), 3.96 (t, ^3J(H,H) = 6.0 Hz, 4H; OCH_2 (thread)), 3.69 (d, ^2J(H,H) = 15.8 Hz, 4H; H4), 3.51 (m, 4H; H6), 3.32 (bt, 4H; $BipyCH_2$), 2.80 (m, 4H; H6), 1.74 (q, ^3J(H,H) = 7.2 Hz, 4H; CH_2 (thread)), 1.36 (s, 36H; CCH_3), 1.31 (q, ^3J(H,H) = 6.1 Hz, 4H; CH_2 (thread)), 0.99 (bs, 4H; CH_2 (thread)), 2.82 ppm (s, 2H; H14); ^{13}C NMR ($CDCl_3$, 125 MHz) $\delta=$158,7, 158.4, 157.0, 152.3, 146.6, 135.8, 133.6, 129.9, 128.4, 128.1, 119.9, 115.2, 115.1, 111.9, 108.7, 84.8, 67.4, 66.9, 64.5, 51.0, 44.4, 31.4, 28.7, 23.0, 22.4 ppm; IR (KBr) $\tilde{\nu}=3443$, 2952, 2868, 1701, 1653, 1592, 1560, 1517, 1490, 1457, 1448, 1426, 1385, 1363, 1298, 1249, 1215, 1142, 1120, 1062, 967, 843, 802, 752, 708, 557 cm^{-1}; MS (MALDI-TOF): *m/z* 2049.5 $[M-2PF_6]^+$.

[2]Rotaxane 19: Porphyrin **1** (10 mg, 7.4 μmol), pyridinium salt **16** (23 mg, 37 μmol) and bromide **13** (118 mg, 296 μmol) were dissolved in DMF (1.5 mL). The resulting solution was stirred overnight at 90 °C under an argon atmosphere. After cooling, the solvent was evaporated and the resulting solid was dissolved in MeCN. To this solution a saturated aqueous solution of NH_4PF_6 was added. Water and $CHCl_3$ were added and the organic layer was separated and evaporated to dryness. The crude mixture was subjected to column chromatography (silica, CH_2Cl_2 to 0.3% MeOH/CH_2Cl_2 (*v/v*) to 0.5% MeOH/CH_2Cl_2 (*v/v*)) to yield **19** as a purple solid (11 mg, 61%). M.p. > 300 °C (decomposed); ^{1}H NMR ($CDCl_3$, 300 MHz) $\delta=9.08$ (s, 4H; H12), 8.77 (s, 4H; H13), 8.10 (dd, ^3J-

(H,H) = 7.4 Hz, ^5J(H,H) = 1.7 Hz, 4H; H11), 7.82 (dt, ^3J(H,H) = 8.0 Hz, ^5J(H,H) = 1.7 Hz, 4H; H10), 7.44 (t, ^3J(H,H) = 7.4 Hz, 4H; H9), 7.41 (d, ^3J(H,H) = 8.5 Hz, 4H; H8), 7.05 (t, ^5J(H,H) = 1.5 Hz, 2H; *para*-ArH (thread)), 7.04–6.97 (m, 6H; H1, H2), 6.94–6.89 (m, 4H; H3), 6.85 (d, ^5J-(H,H) = 1.6 Hz, 4H; *ortho*-ArH (thread)), 6.13 (d, ^3J(H,H) = 6.1 Hz, 4H; BipyH), 6.07 (s, 4H; H5), 4.90 (d, ^3J(H,H) = 6.1 Hz, 4H; BipyH), 4.40–4.35 (m, 4H; H7), 4.28 (d, ^2J(H,H) = 15.9 Hz, 4H; H4), 4.05–3.95 (m, 4H; H7), 4.05 (t, ^3J(H,H) = 6.0 Hz, 4H; OCH_2 (thread)), 3.73 (d, ^2J-(H,H) = 15.8 Hz, 4H; H4), 3.56–3.46 (m, 4H; H6), 3.32 (bt, 4H; $BipyCH_2$), 2.82–2.73 (m, 4H; H6), 1.85 (q, ^3J(H,H) = 7.2 Hz, 4H; CH_2 (thread)), 1.60–1.50 (m, 4H; CH_2 (thread)), 1.42–1.20 (m, 8H; CH_2 (thread)), 1.35 (s, 36H; CCH_3), 1.10 (bs, 4H; CH_2 (thread)), 0.94 (bs, 4H; CH_2 (thread)), −2.82 ppm (s, 2H; H14); ^{13}C NMR ($CDCl_3$, 125 MHz) δ = 158.7, 158.5, 158.2, 152.2, 146.2, 145.0, 142.5, 135.6, 132.7, 131.2, 130.6, 130.1, 129.1, 128.8, 128.0, 126.0, 123.2, 121.5, 120.5, 116.5, 114.8, 112.2, 85.4, 68.4, 67.6, 67.3, 64.3, 61.7, 50.8, 44.0, 43.5, 35.0, 31.5, 29.5, 29.1, 28.9, 28.8, 26.1, 26.0 ppm. IR (KBr) $\tilde{\nu}$ = 3455, 2951, 2862, 1701, 1636, 1594, 1521, 1473, 1363, 1301, 1249, 1217, 1121, 1061, 968, 845, 708, 558 cm^{-1}; MS (MALDI-TOF): *m*/*z* 2280.6 $[M-PF_6]^+$, 2135.6 $[M-2PF_6]^+$.

[2]Rotaxane 20: Compounds **14** (22 mg, 50 μmol), **17** (22 mg, 33 μmol) and **1** (8.5 mg, 6.3 μmol) were suspended in argon-flushed DMF (3 mL). The mixture was heated under argon at 120 °C for 5 days. After cooling, the product was dissolved in $CHCl_3$ (5 mL). A saturated aqueous NH_4PF_6 solution (5 mL) was added and the mixture was stirred vigorously for 2 h. The organic layer was separated, washed with water, and evaporated to dryness. The crude product was purified by column chromatography (first column: Silica 60H, 2% MeOH in $CHCl_3$, *v*/*v*; second column: size exclusion, toluene) to give **20** (6 mg, 38%) as a purple solid. M.p. > 300 °C (decomposed); ^{1}H NMR ($CDCl_3$, 300 MHz) δ = 9.07 (s, 4H; H12), 8.79 (s, 4H; H13), 8.11 (dd, ^3J(H,H) = 7.4 Hz, ^5J(H,H) = 1.7 Hz, 4H; H11), 7.83 (dt, ^3J(H,H) = 8.0 Hz, ^5J(H,H) = 1.7 Hz, 4H; H10), 7.46 (t, ^3J(H,H) = 7.4 Hz, 4H; H9), 7.42 (d, ^3J(H,H) = 8.5 Hz, 4H; H8), 7.03 (t, ^5J-(H,H) = 1.5 Hz, 2H; *para*-ArH (thread)), 7.05–6.99 (m, 6H; H1, H2), 6.95–6.88 (m, 4H; H3), 6.81 (d, ^5J(H,H) = 1.6 Hz, 4H; *ortho*-ArH (thread)), 6.14 (d, ^3J(H,H) = 6.1 Hz, 4H; BipyH), 6.08 (s, 4H; H5), 4.89 (bs, 4H; BipyH), 4.39–4.30 (m, 4H; H7), 4.28 (d, ^2J(H,H) = 15.9 Hz, 4H; H4), 4.10–4.00 (m, 4H; H7), 4.03 (t, ^3J(H,H) = 6.0 Hz, 4H; OCH_2 (thread)), 3.74 (d, ^2J(H,H) = 15.8 Hz, 4H; H4), 3.58–3.49 (m, 4H; H6), 3.32 (bs, 4H; $BipyCH_2$), 2.84–2.75 (m, 4H; H6), 1.87–0.8 (m, 36H; CH_2 (thread)) 1.33 (s, 36H; CCH_3), −2.81 ppm (s, 2H; H14); ^{13}C NMR ($CDCl_3$, 125 MHz) δ = 158.7, 152.1, 146.2, 145.2, 142.4, 135.6, 132.9, 131.2, 130.6, 130.2, 128.7, 128.1, 123.5, 120.4, 116.6, 116.4, 114.8, 112.2, 108.8, 85.4,68.5, 67.8, 67.4, 44.0, 35.0, 31.5, 30.4, 29.6, 29.4, 28.8, 26.3 ppm; IR (KBr) $\tilde{\nu}$ = 3455, 2957, 2871, 1700, 1663, 1558, 1545, 1436, 1419, 1384, 1248, 1121, 1064, 968, 844, 668, 558 cm^{-1}; MS (MALDI-TOF): *m*/*z* 2364.3 $[M-PF_6]^+$, 2219.4 $[M-2PF_6]^+$.

Acknowledgements

This research was supported by the European Research Council in the form of an ERC Starting grant for J.A.A.W.E (NANOCAT-259064) and an ERC Advanced grant for R.J. M.N. (ALPROS-290886). The Dutch National Research School for Combination Catalysis (NRSC-C) is acknowledged for financial support to R.G.E.C and R.J.M.N. Further financial support was obtained from the Council for the Chemical Sciences of the Netherlands Organization for Scientific Research (CW-NWO) (Vidi grant for J.A.A.W.E and Vici grant for A.E.R) and from the Ministry of Education, Culture and Science (Gravity program 024.001.035).

[1] a) K. Kim, *Chem. Soc. Rev.* **2002**, *31*, 96; b) S. J. Cantrill, K. S. Chichak, A. J. Peters, J. F. Stoddart, *Acc. Chem. Res.* **2005**, *38*, 1; c) J. D. Crowley, S. M. Goldup, A.-L. Lee, D. A. Leigh, R. T. McBurney, *Chem. Soc. Rev.* **2009**, *38*, 1530; d) R. S. Forgan, J.-P. Sauvage, J. F. Stoddart, *Chem. Rev.* **2011**, *111*, 5434; e) *From Non-covalent Assemblies to Molecular Machines* (Eds.: J.-P. Sauvage and P. Gaspard), Wiley-VCH, Weinheim, **2011**; f) C.-F. Chang, C.-J. Chuang, C.-C. Lai, Y.-H. Liu, S.-M. Peng, S.-H. Chiu, *Angew. Chem.* **2012**, *124*, 10241; *Angew. Chem. Int. Ed.* **2012**, *51*, 10094.

[2] a) C. P. Collier, G. Mattersteig, E. W. Wong, Y. Luo, K. Beverly, J. Sampaio, F. M. Raymo, J. F. Stoddart, J. R. Heath, *Science* **2000**, *289*, 1172; b) Y. Luo, C. P. Collier, J. O. Jeppesen, K. A. Nielsen, E. Delonno, G. Ho, J. Perkins, H. R. Tseng, T. Yamamoto, J. F. Stoddart, J. R. Heath, *ChemPhysChem* **2002**, *3*, 519.

[3] a) T. J. Huang, B. Brough, C. M. Ho, Y. Liu, A. H. Flood, P. A. Bonvallet, H. R. Tseng, J. F. Stoddart, M. Baller, S. Magonov, *Appl. Phys. Lett.* **2004**, *85*, 5391; b) Y. Liu, A. H. Flood, P. A. Bonvallett, S. A. Vignon, B. H. Northrop, H. R. Tseng, J. O. Jeppesen, T. J. Huang, B. Brough, M. Baller, S. Magonov, S. D. Solares, W. A. Goddard, C. M. Ho, J. F. Stoddart, *J. Am. Chem. Soc.* **2005**, *127*, 9745.

[4] Interlocked molecules are not the only excellent candidates for the bottom-up approach in nanotechnology, for example, see: a) N. Koumura, R. W. J. Zijlstra, R. A. van Delden, N. Harada, B. L. Feringa, *Nature* **1999**, *401*, 152; b) V. Balzani, A. Credi, F. M. Raymo, J. F. Stoddart, *Angew. Chem.* **2000**, *112*, 3484; *Angew. Chem. Int. Ed.* **2000**, *39*, 3348; c) K. Kinbara, T. Aida, *Chem. Rev.* **2005**, *105*, 1377; d) A. Kocer, M. Walko, W. Meijberg, B. L. Feringa, *Science* **2005**, *309*, 755. W. R. Browne, B. L. Feringa, *Nat. Nanotechnol.* **2006**, *1*, 25; e) K. Miwa, Y. Furusho, E. Yashima, *Nat. Chem.* **2010**, *2*, 444.

[5] A. M. Turing, *Proc. London Math. Soc.* **1937**, 42, 230.

[6] a) P. Thordarson, E. J. A. Bijsterveld, A. E. Rowan, R. J. M. Nolte, *Nature* **2003**, *424*, 915; b) C. Monnereau, P. Hidalgo Ramos, A. B. C. Deutman, J. A. A. W. Elemans, R. J. M. Nolte, A. E. Rowan, *J. Am. Chem. Soc.* **2010**, *132*, 1529.

[7] P. Thordarson, R. G. E. Coumans, J. A. A. W. Elemans, P. J. Thomassen, J. Visser, A. E. Rowan, R. J. M. Nolte, *Angew. Chem.* **2004**, *116*, 4859; *Angew. Chem. Int. Ed.* **2004**, *43*, 4755.

[8] a) R. G. E. Coumans, J. A. A. W. Elemans, R. J. M. Nolte, A. E. Rowan, *Proc. Natl. Acad. Sci. USA* **2006**, *103*, 19647; b) P. Hidalgo Ramos, R. G. E. Coumans, A. B. C. Deutman, R. de Gelder, J. M. M. Smits, J. A. A. W. Elemans, R. J. M. Nolte, A. E. Rowan, *J. Am. Chem. Soc.* **2007**, *129*, 5699; c) A. B. C. Deutman, C. Monnereau, J. A. A. W. Elemans, G. Ercolani, R. J. M. Nolte, A. E. Rowan, *Science* **2008**, *322*, 1668.

[9] R. G. E. Coumans, J. A. A. W. Elemans, P. Thordarson, R. J. M. Nolte, A. E. Rowan, *Angew. Chem.* **2003**, *115*, 674; *Angew. Chem. Int. Ed.* **2003**, *42*, 650.

[10] J. A. A. W. Elemans, M. B. Claase, P. P. M. Aarts, A. E. Rowan, A. P. H. J. Schenning, R. J. M. Nolte, *J. Org. Chem.* **1999**, *64*, 7009.

[11] a) B. Mohr, J.-P. Sauvage, R. H. Grubbs, M. Weck, *Angew. Chem.* **1997**, *109*, 1365; *Angew. Chem. Int. Ed. Engl.* **1997**, *36*, 1308; b) T. J. Kidd, D. A. Leigh, A. J. Wilson, *J. Am. Chem. Soc.* **1999**, *121*, 1599; c) P. Mobian, J. M. Kern, J.-P. Sauvage, *J. Am. Chem. Soc.* **2003**, *125*, 2016; d) A. F. M. Kilbinger, S. J. Cantrill, A. W. Waltman, M. W. Day, R. H. Grubbs, *Angew. Chem.* **2003**, *115*, 3403; *Angew. Chem. Int. Ed.* **2003**, *42*, 3281; e) G. Kaiser, S. Jarrosson, S. Otto, Y. F. Ng, A. D. Bond, J. K. M. Sanders, *Angew. Chem.* **2004**, *116*, 1993; *Angew. Chem. Int. Ed.* **2004**, *43*, 1959; f) J. D. Badjić, S. J. Cantrill, R. H. Grubbs, E. N. Guidry, R. Orenes, J. F. Stoddart, *Angew. Chem.* **2004**, *116*, 3335; *Angew. Chem. Int. Ed.* **2004**, *43*, 3273; g) P. G. Clark, E. N. Guidry, W. Y. Chan, W. E. Steinmetz, R. H. Grubbs, *J. Am. Chem. Soc.* **2010**, *132*, 3405; h) V. N. Vukotic, K. J. Harris, K. Zhu, R. W. Schurko, S. J. Loeb, *Nat. Chem.* **2012**, *4*, 456; i) G. T. Spence, P. D. Beer, *Acc. Chem. Res.* **2013**, *46*, 571.

[12] For some examples of other porphyrin containing catenanes, see: a) M. J. Gunter, D. C. R. Hockless, M. R. Johnston, B. W. Skelton, A. H. White, *J. Am. Chem. Soc.* **1994**, *116*, 4810; b) M. Linke, N. Fujita, J. C. Chambron, V. Heitz, J.-P. Sauvage, *New J. Chem.* **2001**, *25*, 790; c) M. J. Gunter, S. M. Farquhar, *Org. Biomol. Chem.* **2003**, *1*, 3450; d) M. Beyler, V. Heitz, J.-P. Sauvage, *Chem. Commun.* **2008**, 5396; e) M. J. Langton, J. D. Matichak, A. L. Thompson, H. L. Anderson, *Chem. Sci.* **2011**, *2*, 1897.

[13] A similar statistical approach to the synthesis of simple molecular necklaces by using Glaser–Hay coupling has been reported, see: F. Bitsch, C. O. Dietrich-Buchecker, J. P. Khemiss, J.-P. Sauvage, A. Van Dorsselaer, *J. Am. Chem. Soc.* **1991**, *113*, 4023.

[14] For some other examples of molecular necklaces, see: a) D. B. Amabilino, P. R. Ashton, J. F. Stoddart, A. J. P. White, D. J. Williams, *Chem. Eur. J.* **1998**, *4*, 460; b) D. Whang, K. M. Park, J. Heo, P. Ashton, K. Kim, *J. Am. Chem. Soc.* **1998**, *120*, 4899; c) Y. H. Ko, K. Kim, J. K. Kang, H. Vhun, J. W. Lee, S. Sakamoto, K. Yamaguchi, J. C. Fettinger, K. Kim, *J. Am. Chem. Soc.* **2004**, *126*, 1932.

[15] M. J. Gunter, M. R. Johnston, *J. Chem. Soc. Chem. Commun.* **1994**, 829.

[16] For some examples of induced motion in interlocked molecules, see: a) A. S. Lane, D. A. Leigh, A. Murphy, *J. Am. Chem. Soc.* **1997**, *119*, 11092; b) P. R. Ashton, R. Ballardini, V. Balzani, I. Baxter, A. Credi, M. C. T. Fyfe, M. T. Gandolfi, M. Gómez-López, M.-V. Martínez-Díaz, A. Piersanti, N. Spencer, J. F. Stoddart, M. Venturi, A. J. P. White, D. J. Williams, *J. Am. Chem. Soc.* **1998**, *120*, 11932; c) A. M. Brouwer, C. Frochot, F. G. Gatti, D. A. Leigh, L. Mottier, F. Paolucci, S. Roffia, G. W. H. Wurpel, *Science* **2001**, *291*, 2124; d) A. Altieri, G. Bottari, F. Dehez, D. A. Leigh, J. K. Y. Wong, F. Zerbetto, *Angew. Chem.* **2003**, *115*, 2398; *Angew. Chem. Int. Ed.* **2003**, *42*, 2296; e) D. A. Leigh, J. K. Y. Wong, F. Dehez, F. Zerbetto, *Nature* **2003**, *424*, 174; f) J. D. Badjic, V. Balzani, A. Credi, S. Silvi, J.-F. Stoddart, *Science* **2004**, *303*, 1845; g) V. Serreli, C.-F. Lee, E. R. Kay, D. A. Leigh, *Nature* **2007**, *445*, 523.

[17] I. O. Sutherland, *Annu. Rep. NMR Spectrosc.* **1972**, *4*, 71.

[18] For some other examples of switchable interlocked molecular machines with fluorescent signals, see: a) Q.-C. Wang, D.-H. Qu, J. Ren, K. Chen, H. Tian, *Angew. Chem.* **2004**, *116*, 2715; *Angew. Chem. Int. Ed.* **2004**, *43*, 2661; b) E. M. Pérez, D. T. F. Dryden, D. A. Leigh, G. Teobaldi, F. Zerbetto, *J. Am. Chem. Soc.* **2004**, *126*, 12210; c) D. A. Leigh, M. A. F. Morales, E. M. Perez, J. K. Y. Wong, C. G. Saiz, A. M. Z. Slawin, A. J. Carmichael, D. M. Haddleton, A. M. Brouwer, W. J. Buma, G. W. H. Wurpel, S. Leon, F. Zerbetto, *Angew. Chem.* **2005**, *117*, 3122; *Angew. Chem. Int. Ed.* **2005**, *44*, 3062.

Received: November 7, 2013
Revised: April 3, 2013
Published online: ■■ ▮▮, 0000

Switchable Molecules

R. G. E. Coumans,
J. A. A. W. Elemans, A. E. Rowan,**
*R. J. M. Nolte** ..... ■■■■–■■■■

Interlocked Porphyrin Switches

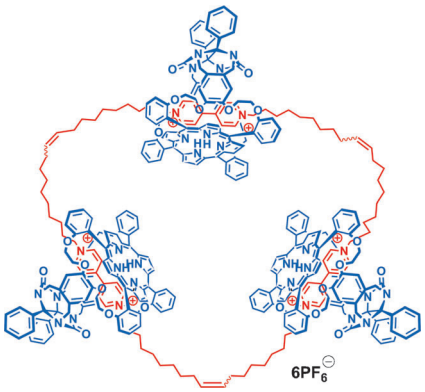

Olefin metathesis is used as an elegant method to construct a series of catenanes and rotaxanes based on olefin-containing viologen threads and cavity-containing porphyrin macrocycles. By varying the olefin substituents of the viologens, the outcome of the metathesis reactions can be controlled. The interlocked porphyrin structures show acid/base-controlled switching behavior (see figure).

